Transit Spectroscopy

Jacob Bean
University of Chicago

Some recent reviews:

- "*Exoplanetary Atmospheres—Chemistry, Formation Conditions, and Habitability*" Madhusudhan+ 2016

- "*Observations of Exoplanet Atmospheres*" Crossfield 2015

Spectral Retrievals

Key references:

- Madhusudhan & Seager 2009
- Benneke & Seager 2012, 2013 ← for super-Earths
- Benneke 2015, arXiv:1504.07655
- Line et al. 2013ac, 2014a, 2016
- Line et al. 2014b, 2015 ← for brown dwarfs
- Lee et al. 2013; Todorv et al. 2016 ←for directly imaged planets
- Barstow et al. 2013ab

Why High Precision Spectroscopy? Effect of the priors

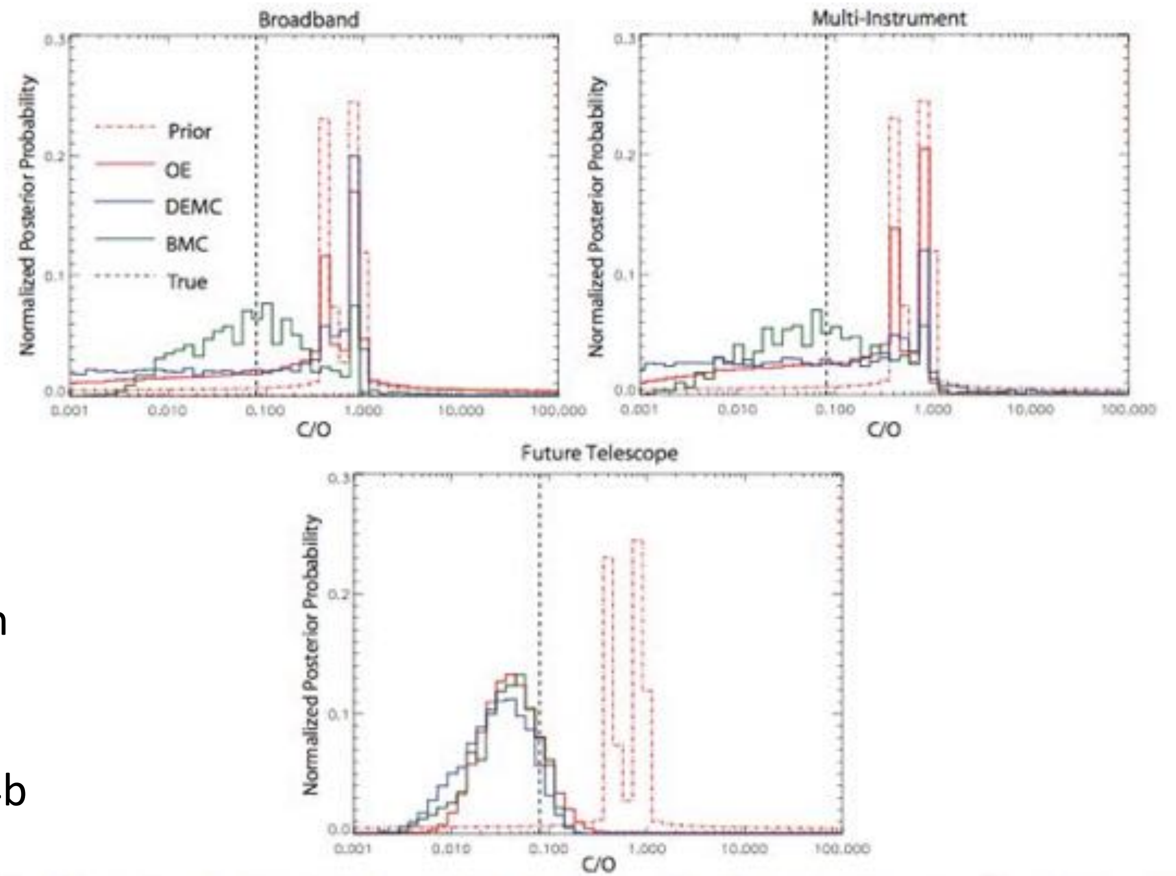

Figure 10. C to O ratio posteriors. The dot-dashed red curve is the prior, the solid red curve is from OE, blue is from DEMC, and green is from BMC. The vertical dashed line is the true C/O. In the top left panel are the C/O's derived from the broadband observational scenario, in the top right are the C/O's derived from the multi-instrument scenario, and in the bottom are the C/O's derived from the future spaceborne telescope scenario. Though it appears that the BMC characterizes the C/O errors well, it is for the wrong reasons. See Section 3.3.3.

"Too few data points in pursuit of too many quantities"

Burrows 2014b

Line+ 2013a

Why High Precision Spectroscopy?
The unknown unknowns

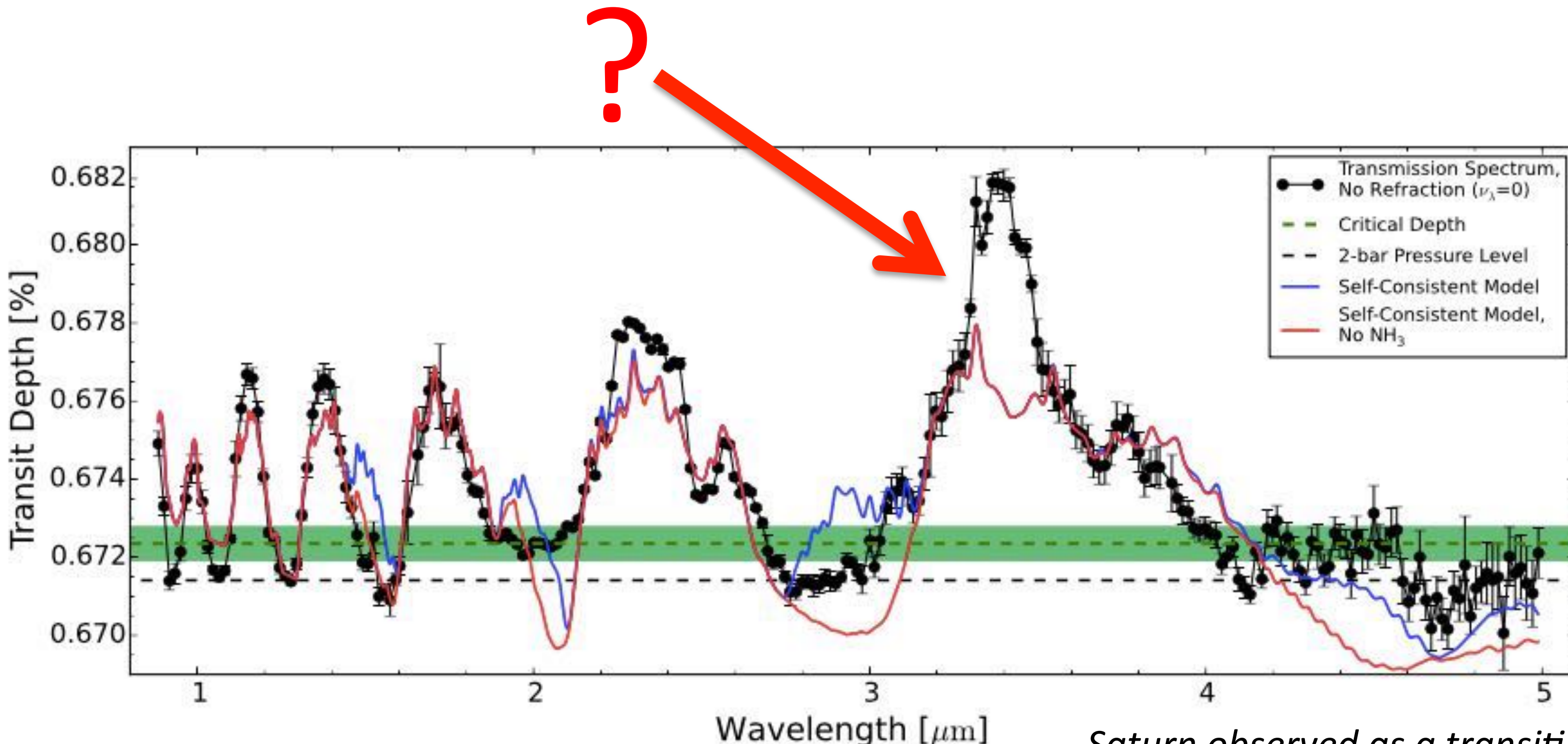

Saturn observed as a transiting exoplanet with Cassini

Dalba+ 2015

Why High Precision Spectroscopy?
I mean, truly high precision data

2 eclipses

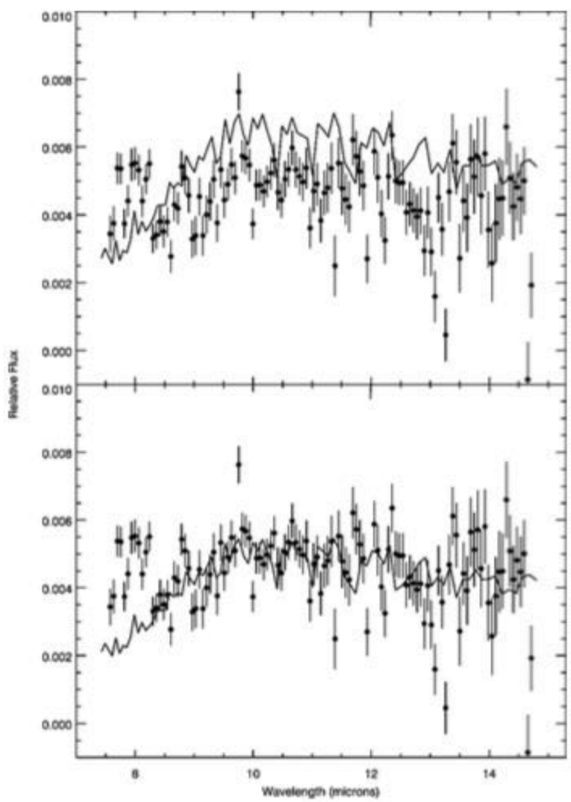

FIG. 3.—Comparison of the flux ratios measured at slit center (*filled circles*) with a model of HD 189733b from Burrows et al. (2006). The model shown is for superior conjunction, with no clouds and 50% energy redistribution to the night side of the planet. The upper panel shows the model as published by Burrows et al. (2006), while in the lower panel the model has been scaled to match the data at $\lambda > 9.5\ \mu m$. Intriguingly, the observed spectrum does not show the expected decrease in relative flux at short wavelengths due to increasing water opacity.

Grillmair+ 2007

10 eclipses

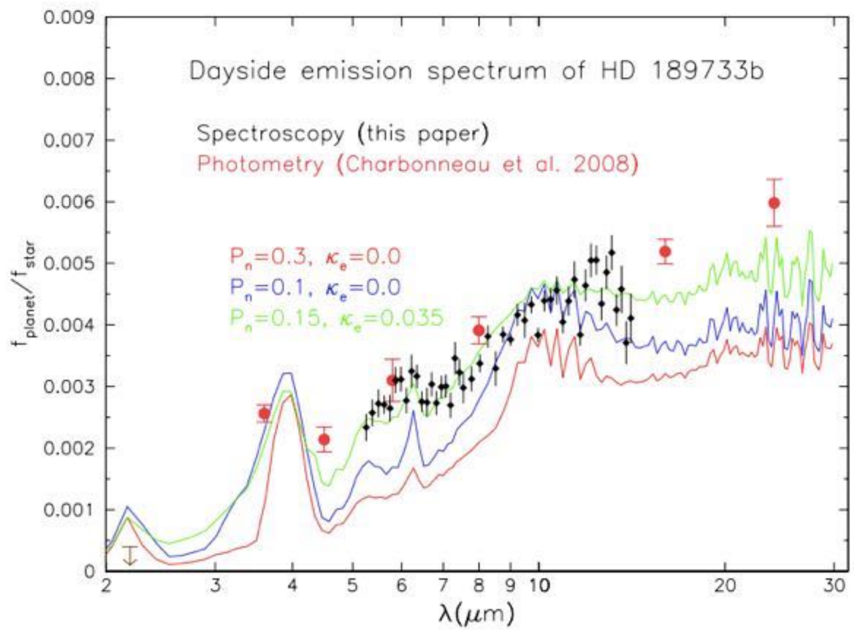

Grillmair+ 2008

Fundamental Themes for Exoplanet Atmosphere Characterization

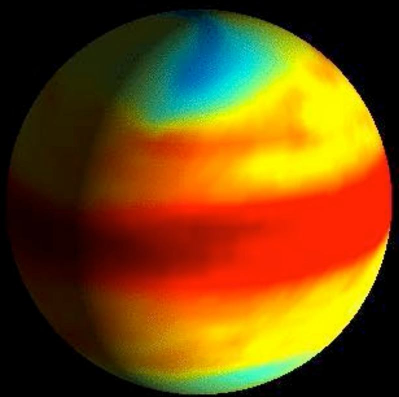

Determining thermal structures, energy budgets, and dynamics to understand planetary physics.

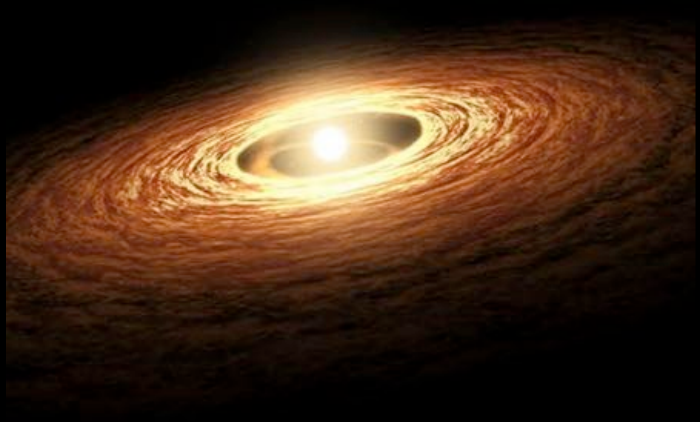

Measuring compositions to trace planet formation and evolution.

Connected questions motivates holistic studies.

Comparative planetology in the Solar System

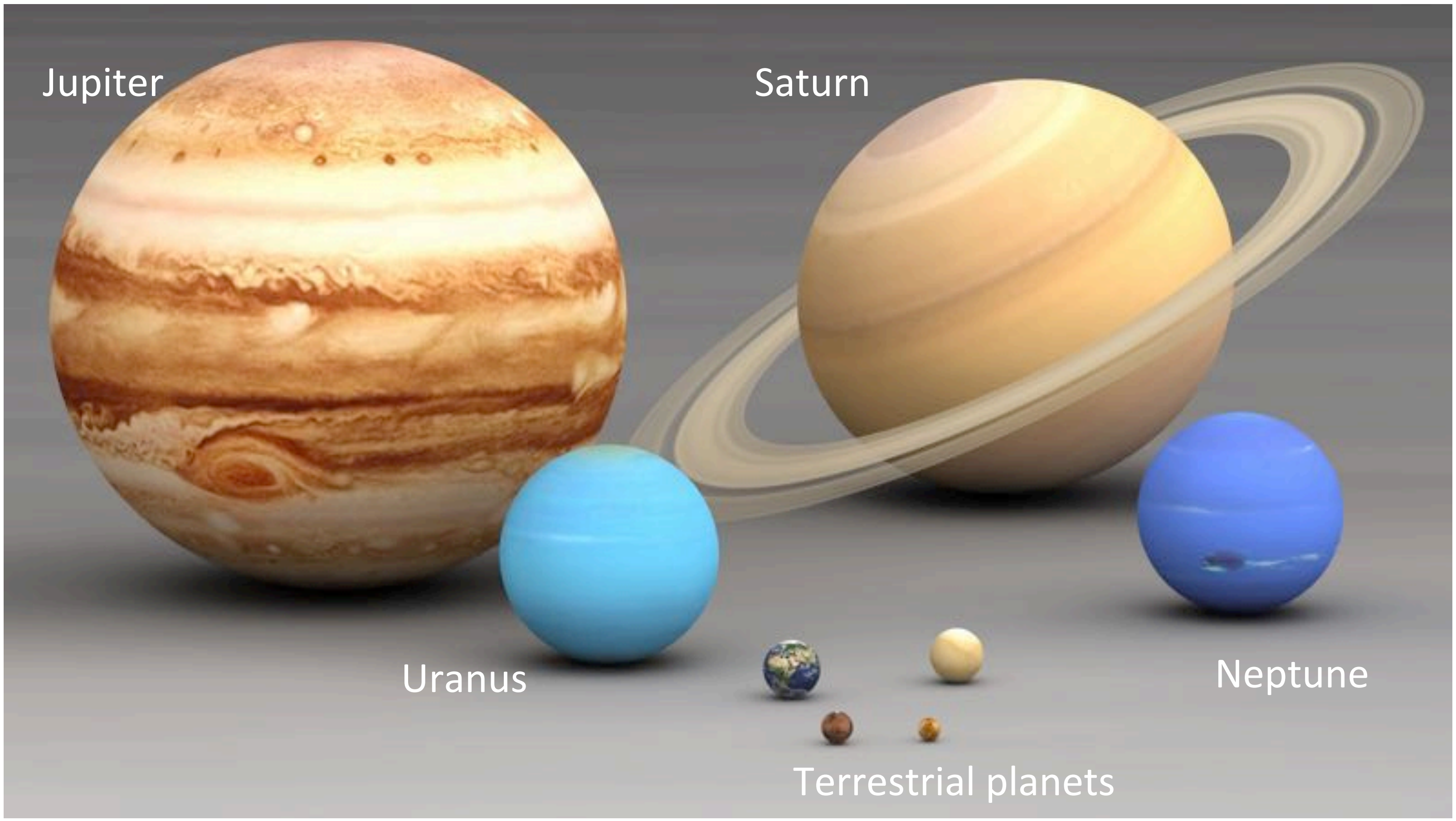

Comparative planetology: Jupiter and Saturn

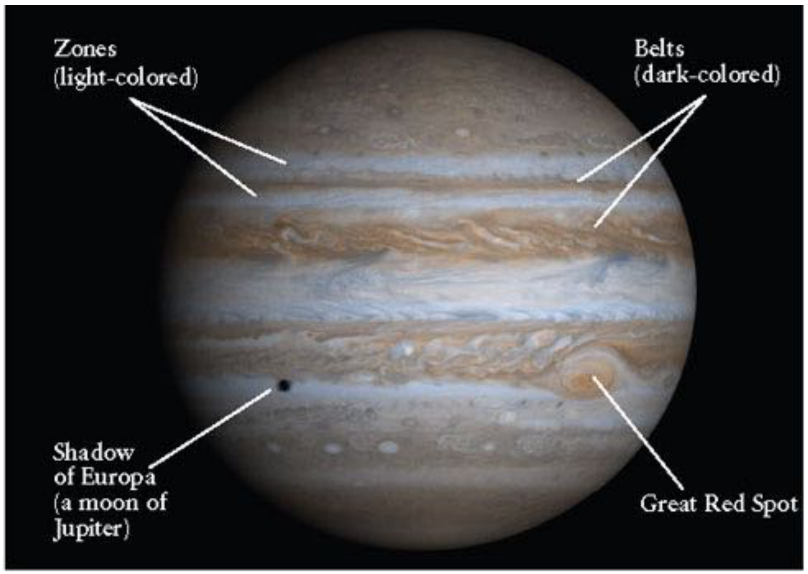

(a) Jupiter

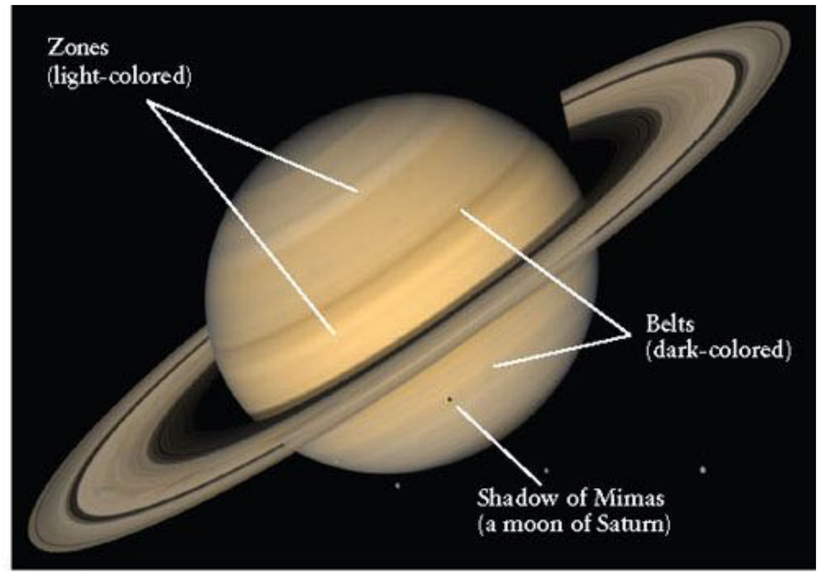

(b) Saturn

Banded appearances due to dynamics of atmosphere: internal heat + fast rotation.

Source of colors is likely complex molecules formed on cloud particles due to photochemistry, but exact nature is uncertain.

Comparative planetology: Jupiter and Saturn

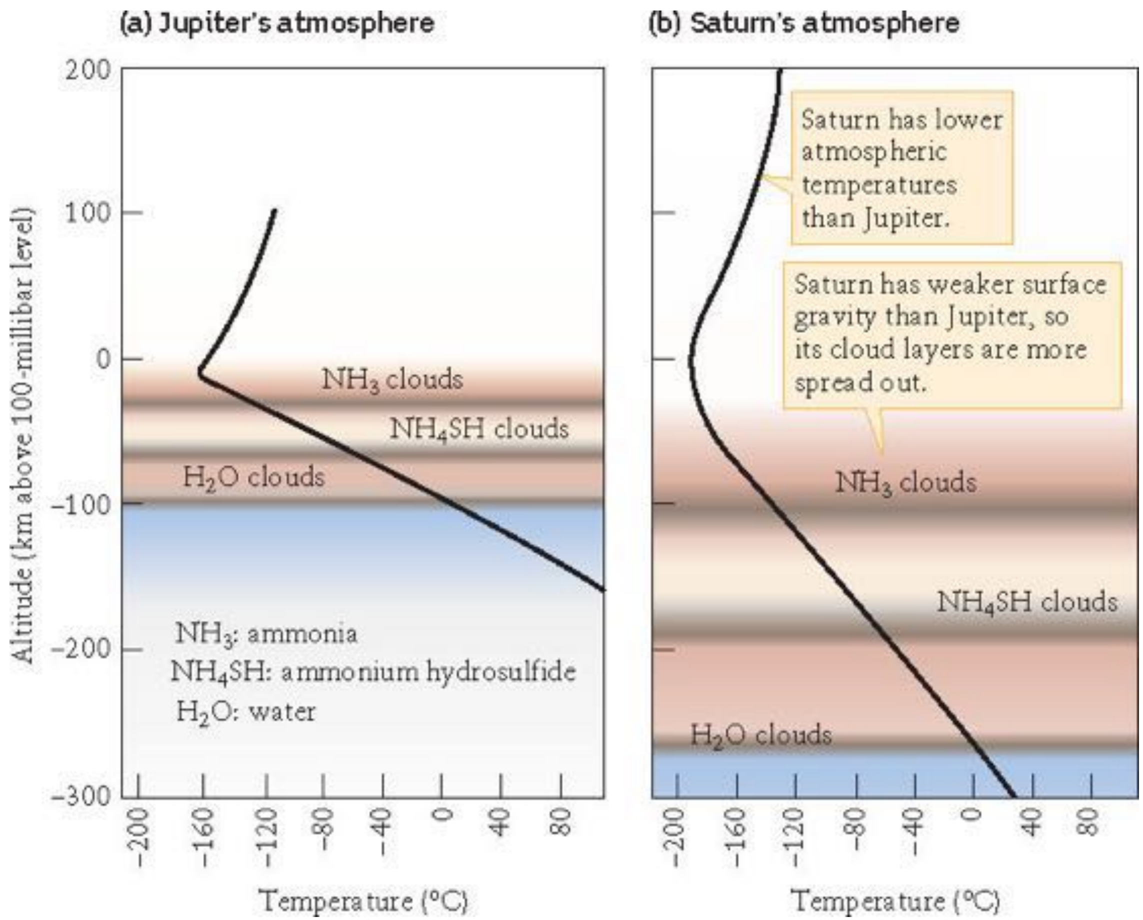

Thinner clouds on Jupiter explains why it has stronger contrast between zones and belts.

Comparative planetology: Uranus and Neptune

Nearly featureless, color due to reflectance of methane.

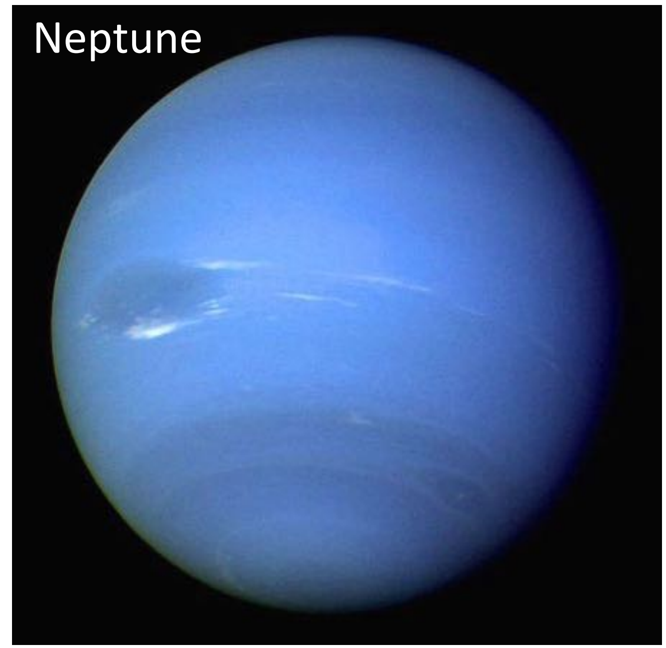

Faint banded structure (slightly faster rotation and internal heat), wispy clouds, and Great Dark Spot.

Comparative planetology: Uranus and Neptune

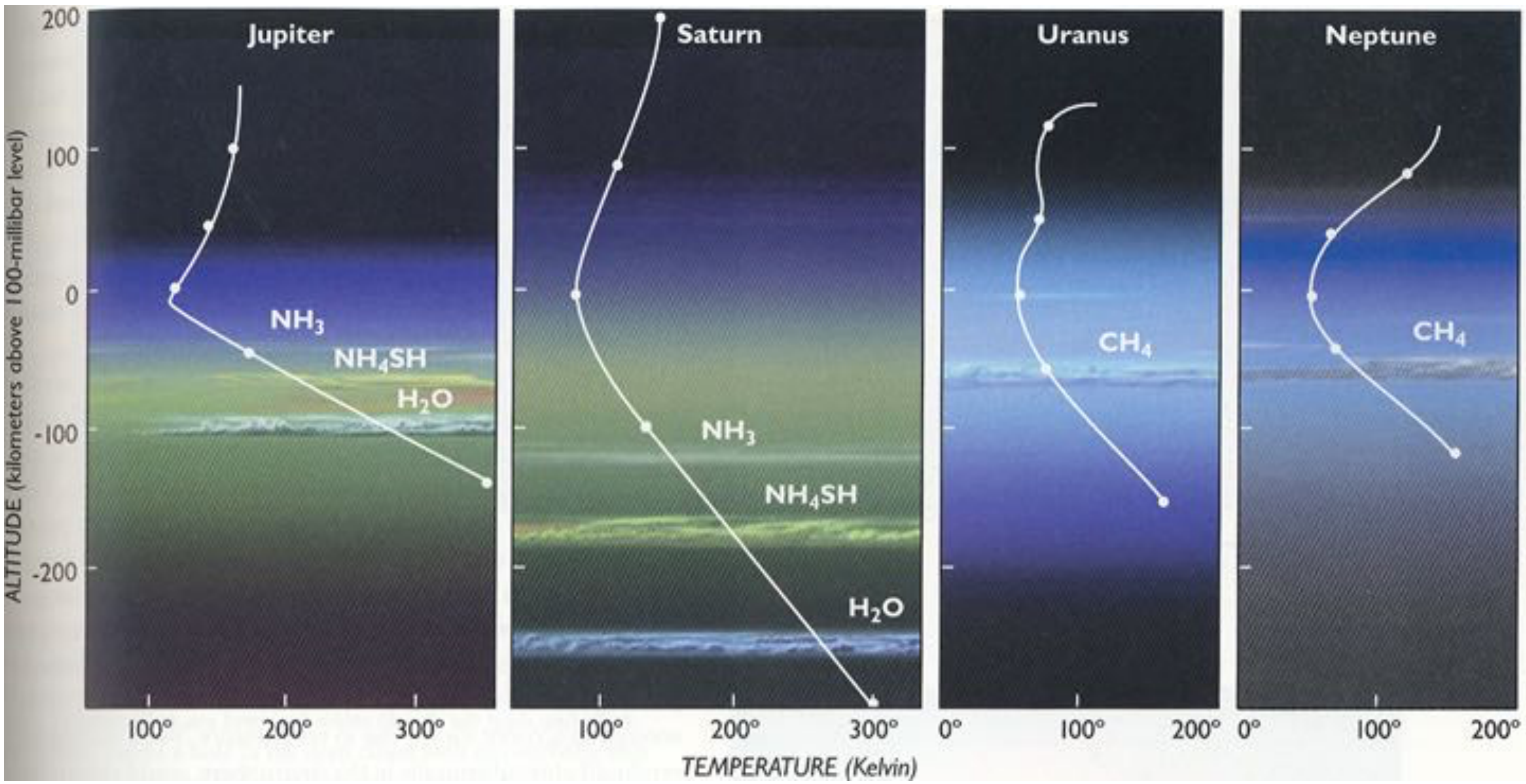

Slight differences between Uranus and Neptune due to internal heat, distance from the Sun, and surface gravity.

Atmospheric Composition

- Giant planet atmospheres are "primary atmospheres".

- Jupiter and Saturn have atmospheric elemental abundances very similar to the Sun (dominated by H/He, with trace heavier elements).

- The atmospheres of Uranus and Neptune are also similar in composition as the Sun, but with a slightly greater enhancement of metals (dominated by H/He, with significant CH_4 and trace heavier elements).

- The abundances in all four planets' atmospheres are strongly affected by condensation:
  - Water in all the planets is not observable because it has settled out of the upper atmosphere.
  - Clouds dominate the appearances of the planets.
  - Helium is deficient in Jupiter's and Saturn's upper atmospheres, likely because it is raining out.

- Non-equilibrium effects (photochemistry, vertical mixing) are significant.

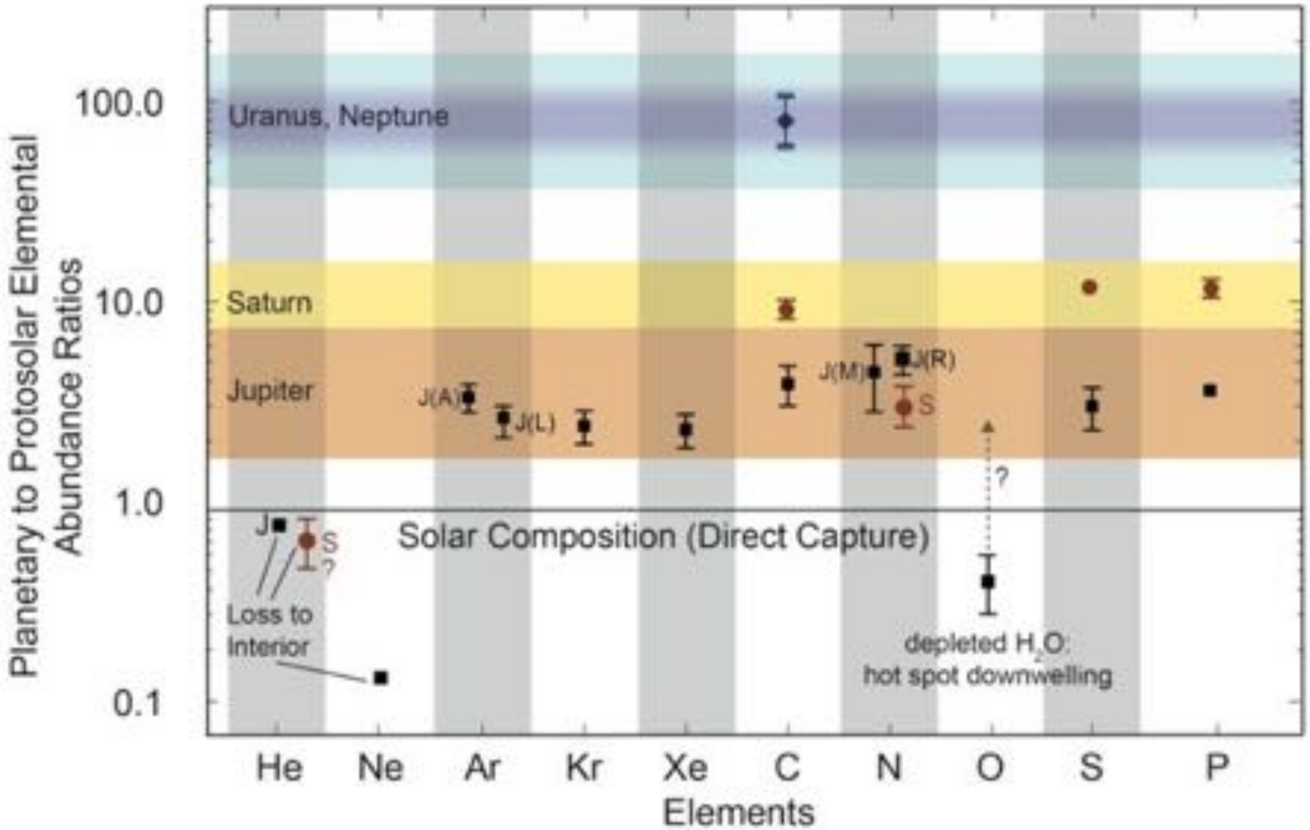

Figure 2.1. Abundances of key elements in the atmospheres of Saturn (brown dots, and label S) and Jupiter (black squares) relative to *protosolar* values derived from the present-day photospheric values of Asplund et al. (2009). Only C/H is presently determined for Uranus and Neptune, though poorly; its best estimate from earth-based observations is shown. The values are listed in Table 2.1. All values are ratioed to H (multiply by 2 for ratio to H_2). Direct gravitational capture would result in solar composition, i.e. no volatile enrichment, hence they would all fall on the horizontal line (normalized to solar) in the middle of the figure. Only He, C, N, S and P have been determined for Saturn, but only C/H is robust for the well-mixed atmosphere (see text). The Jupiter values are from the Galileo probe mass spectrometer (GPMS), except for N/H that was measured by both the GPMS [J(M)] and from attenuation of the probe radio signal through the atmosphere [J(R)]. For Ar, enrichments using both Asplund et al. [J(A)] and Lodders et al. [J(L)] solar values are shown. O/H is sub-solar in the very dry entry site of the Galileo Probe at Jupiter, but was still on the rise at the deepest level probed. Helium is depleted in the shallow troposphere due to condensation and differentiation in the planetary interior. Ne was also depleted in Jupiter as neon vapor dissolves in helium droplets.

Atreya+, arXiv:1606.04510

Terrestrial Planet Atmospheres

				
Planet	Mercury	Venus	Earth	Mars
T_P, K (°C)	437 (163)	232 (-41)	255 (-18)	209 (-64)
T_{obs}, K (°C)	~440 (167)	735 (462)	288 (15)	215 (-58)
Atmosphere: Pressure, kPa composition [trace gases]	none	9300 CO_2(0.965), N_2(0.035), [SO_2, Ar]	101 N_2(0.78), O_2(0.21), Ar(0.009), [CO_2, H_2O]	0.64 CO_2(0.95), N_2(0.03), Ar(0.02), [O_2, CO]

"Secondary atmospheres" strongly influenced by mass loss, geophysical and biological processes, etc.

How To Observe Exoplanet Atmospheres

- Transits/Occultations
- Direct Imaging

Transits and Occultations

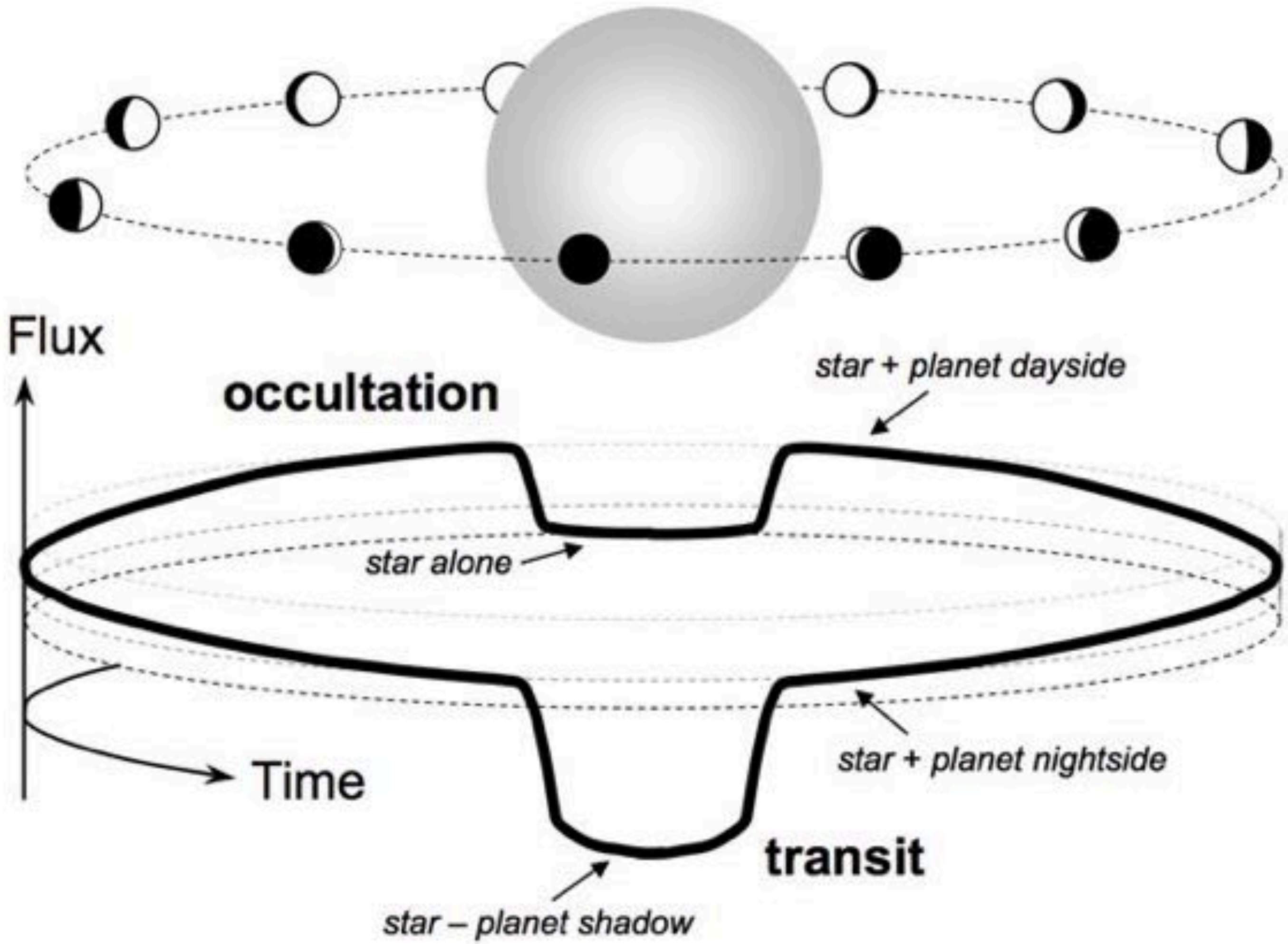

Transits: Emission Spectroscopy

What is measured is the planet-to-star flux ratio:

If reflected light dominates: $F_p/F_s = A_G (R_p/a)^2$

(phase function = 1 at secondary eclipse)

If thermal emission dominates: $F_p/F_s = (R_p/R_S)^2 [B_\lambda(T_P)/B_\lambda(T_s)]$

The thermal emission signal in the infrared for a hot Jupiter around a Sun-like star (T_{eq} = 1600K) is on order of 10^{-3}.

Transits: Emission Spectroscopy

Theoretical predictions for highly-irradiated planets

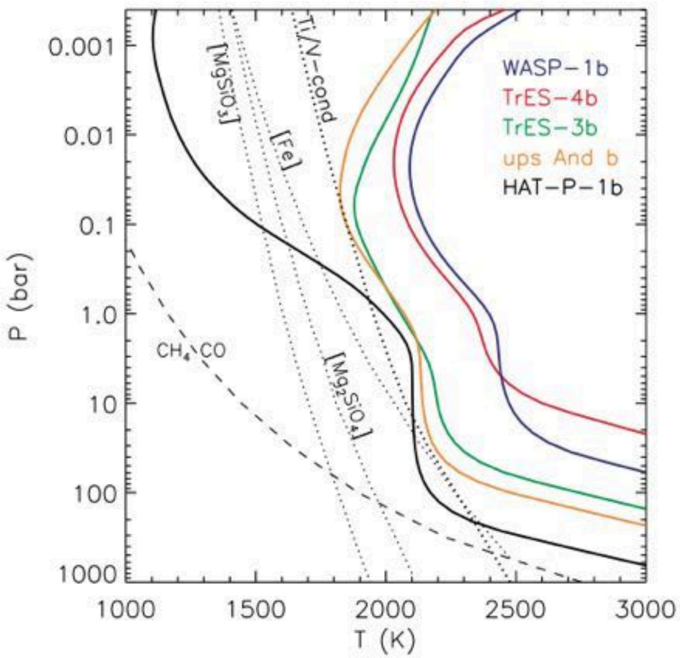

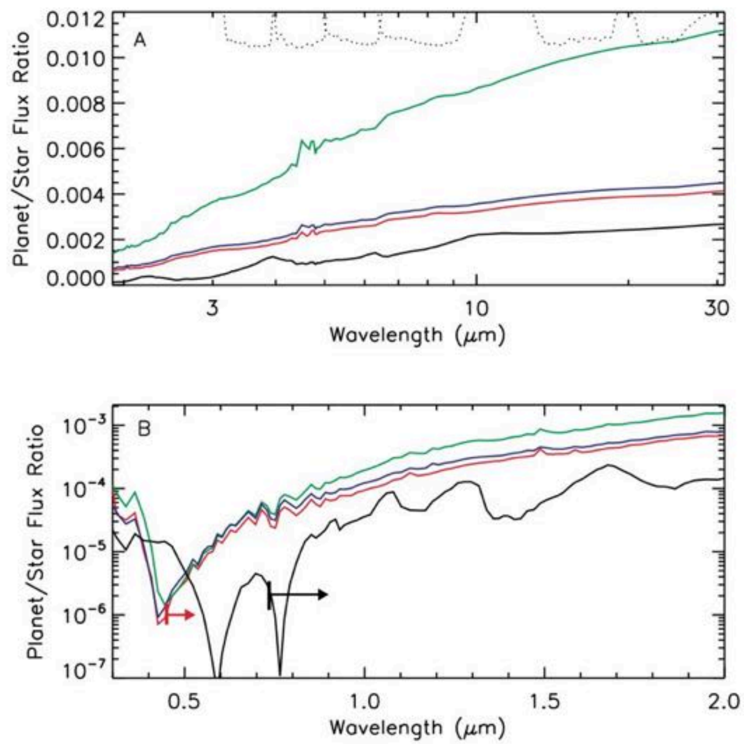

Fortney et al. 2008, ApJ, 678, 1419

Transits: Emission Spectroscopy

Ground-based, short-wavelength, faint star

WASP-19b

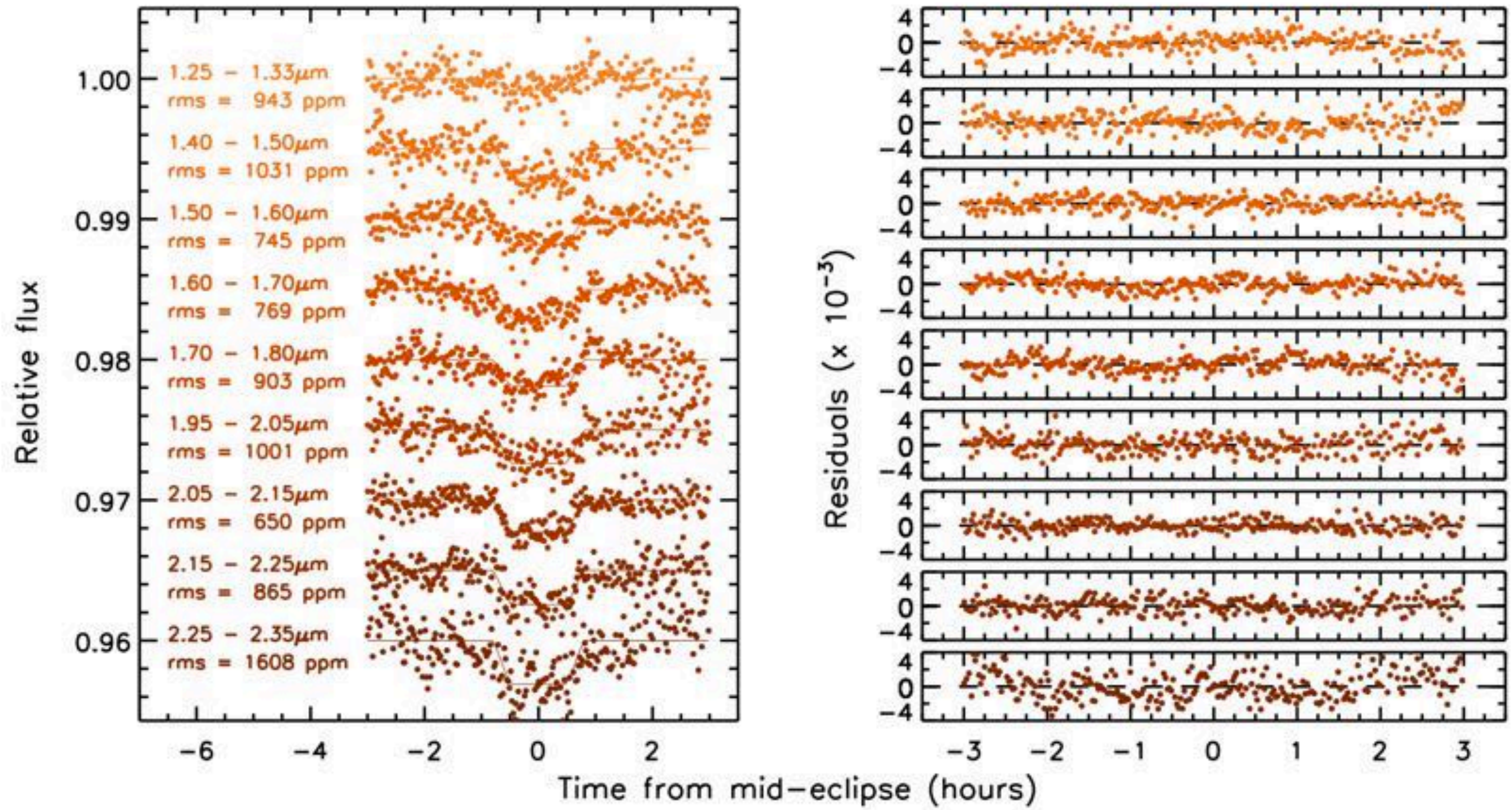

Bean et al. 2013, ApJ, 771, 108

Transits: Emission Spectroscopy

Space-based, longer-wavelength (3.6 and 4.5 μm), bright star

Spitzer Space Telescope

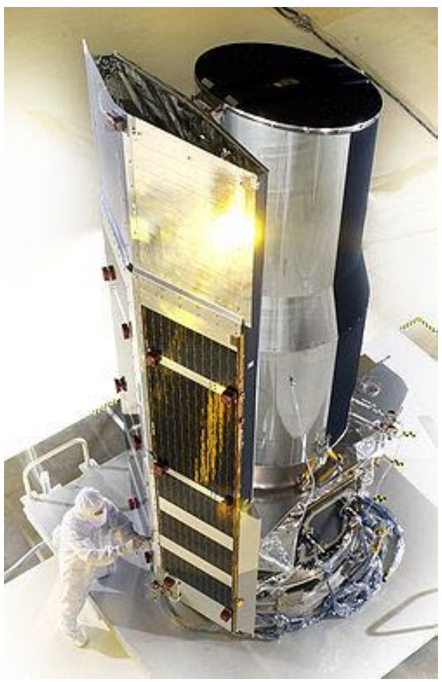

Previous sensitivity to longer wavelengths, but no longer.

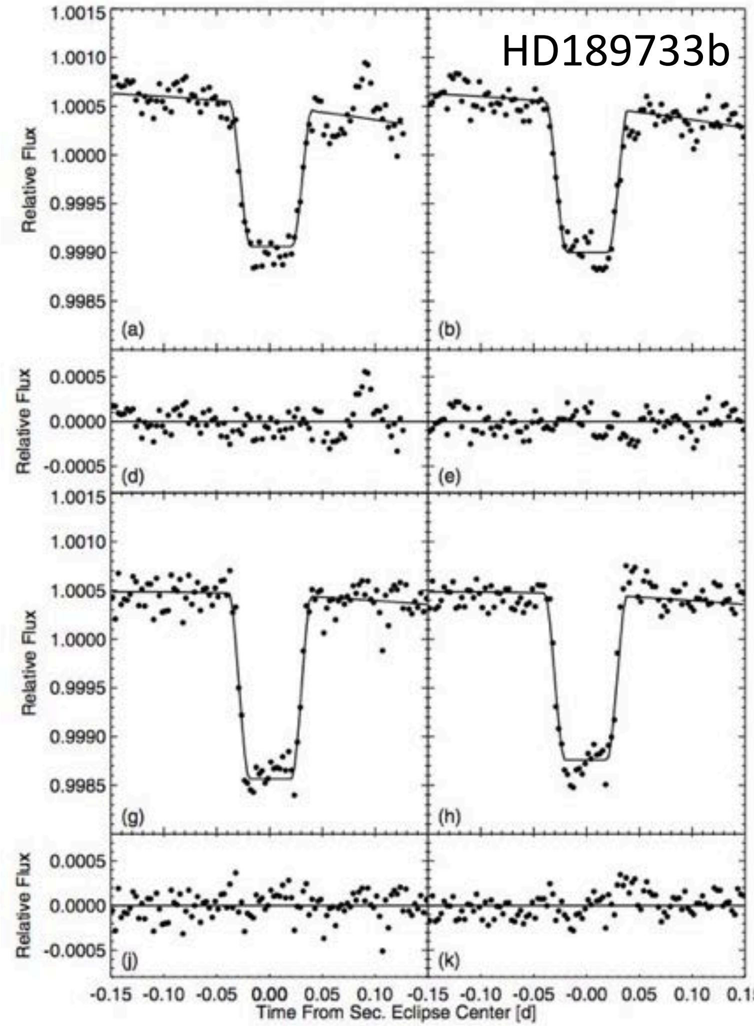

Knutson et al. 2012, ApJ, 754, 22

Transits: Emission Spectroscopy

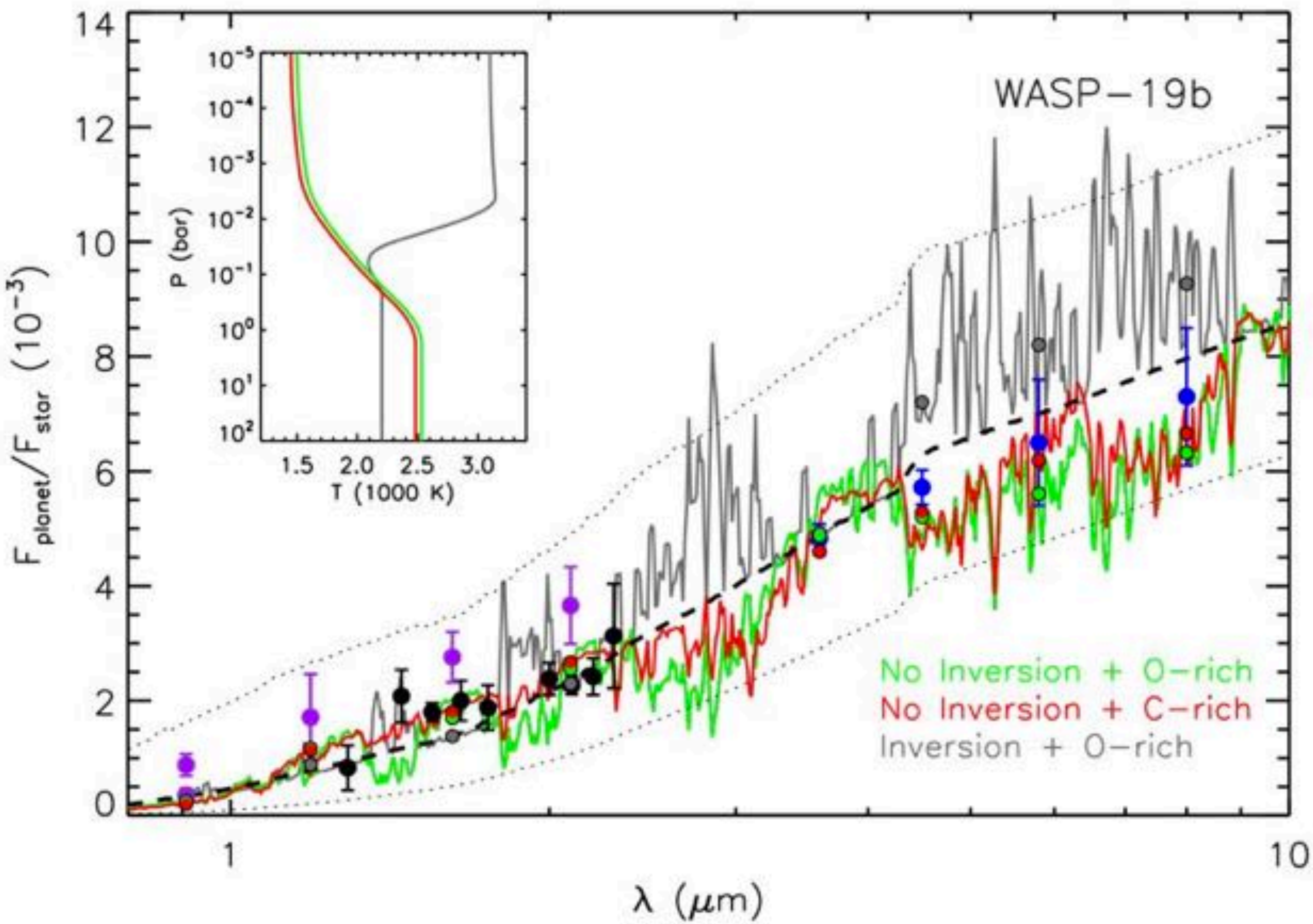

Bean et al. 2013, ApJ, 771, 108

Transits and Occultations

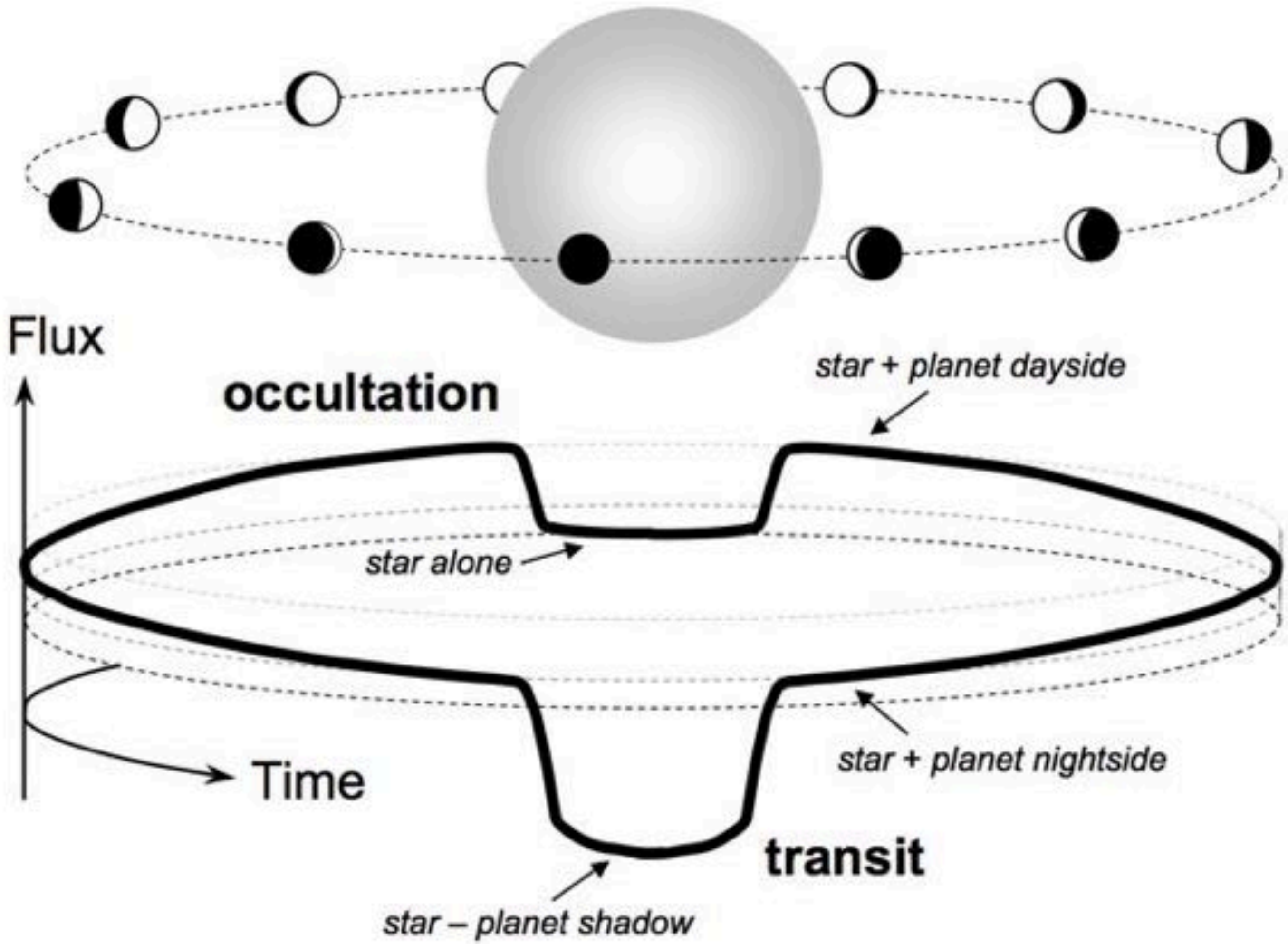

Transits: Transmission Spectroscopy

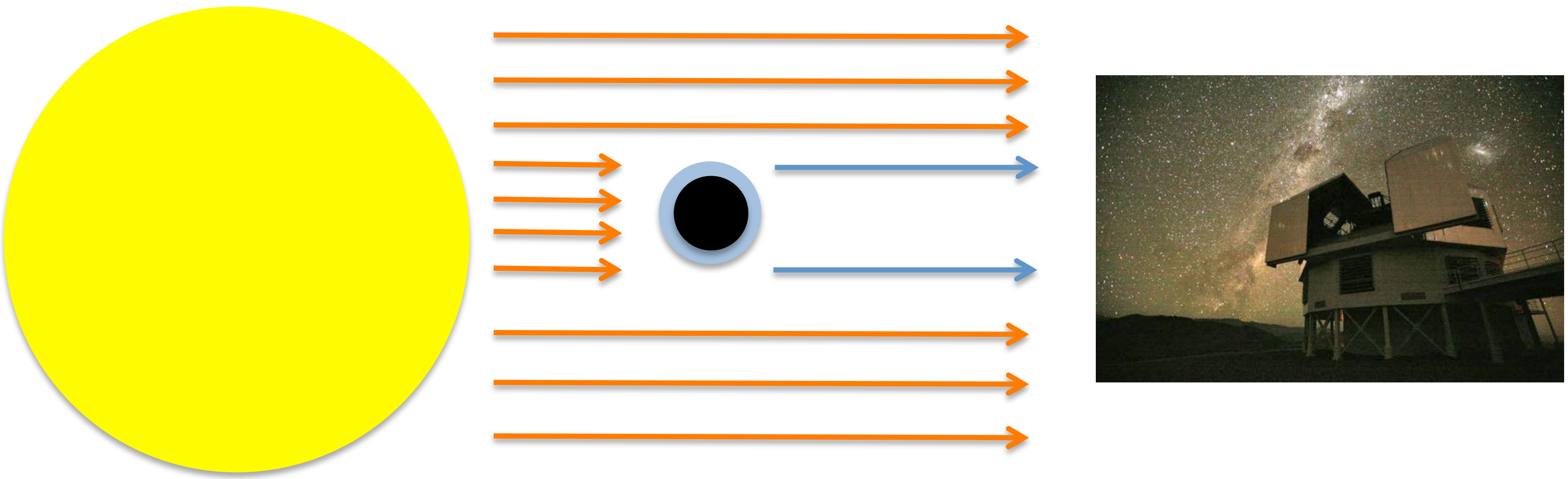

The key point is that the edge of the planet is 'fuzzy' rather than sharp due to the atmosphere.

Therefore, the transit depth (apparent size of the planet) depends on the wavelength of light.

Transits: Transmission Spectroscopy

Theoretical predictions

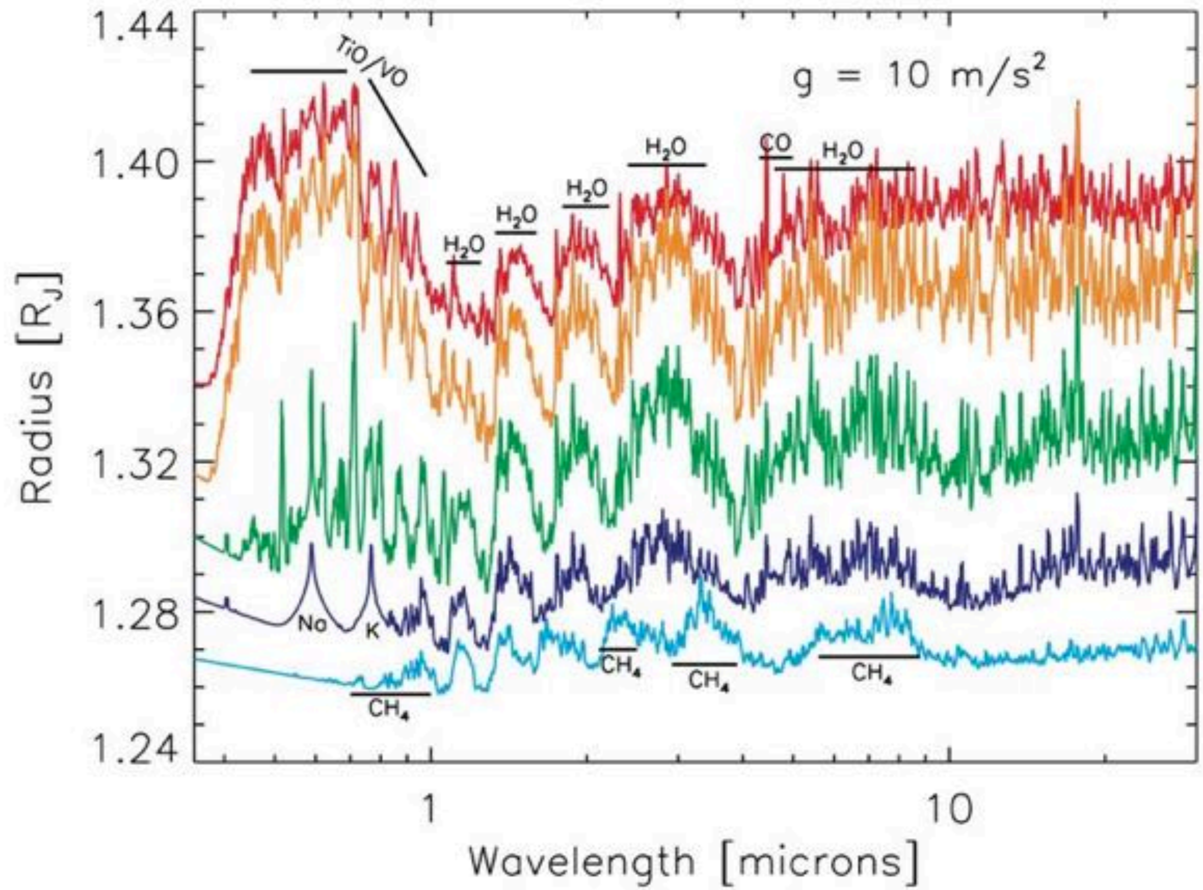

T =
2500 K
2000 K
1500 K
1000 K
500 K

Fortney et al. 2010, ApJ, 709, 1396

Transits: Transmission Spectroscopy

GJ1214b

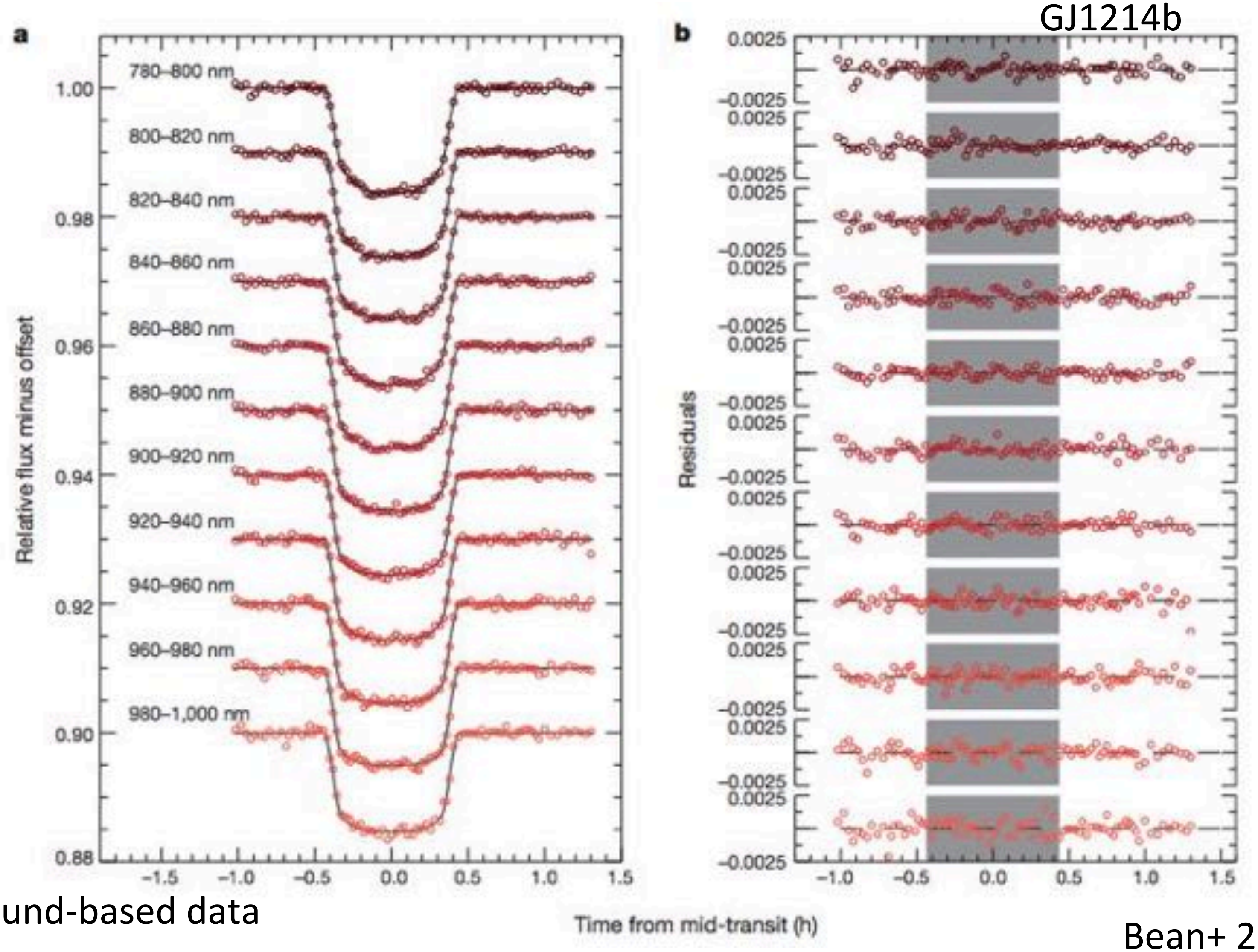

Ground-based data

Bean+ 2010c

Transits: Transmission Spectroscopy

Strength of features in a transmission spectrum depend on the scale height of the atmosphere and the strength of the absorber.

Scale height: $$H = \frac{kT}{\mu_m g}$$

Strength of features:

$$\Delta D \sim \frac{2H R_{\rm pl}}{R_*^2}$$

Where the proportionality factor depends on the strength of absorption (e.g., a factor of a few) and the resolution

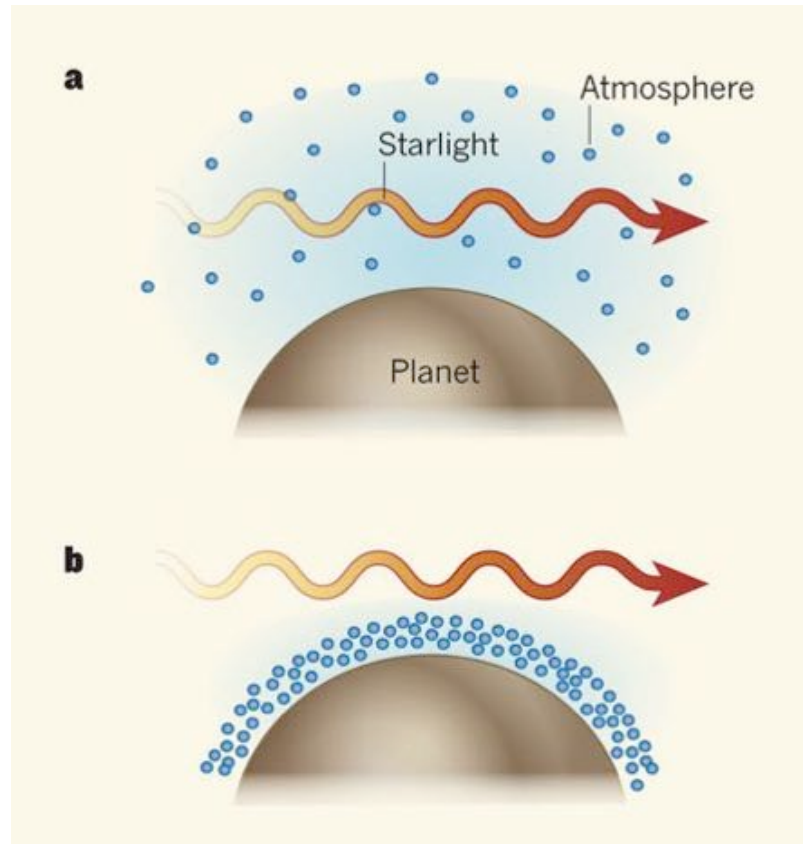

Transits: Transmission Spectroscopy

More precisely:

The atmospheric altitude, $z(\lambda)$, that can be ascribed to the observed absorption as a function of wavelength in a transmission spectrum, is given by the equation from Lecavelier des Etangs et al. (2008a):

$$z(\lambda) = \frac{kT}{\mu g} \ln \left(\frac{\xi \sigma(\lambda) P_o}{\tau_{\rm eq}} \left(\frac{2\pi R_{\rm P}}{kT\mu g} \right)^{1/2} \right), \qquad (3)$$

where k is Boltzmann's constant, T is the temperature, μ is the mean molecular weight of the atmospheric composition, g is the surface gravity, ξ is the ~~elemental abundance,~~ $\sigma(\lambda)$ is the wavelength dependent absorption cross-section, P_o is the pressure at the reference zero altitude, $\tau_{\rm eq}$ is the optical depth at the transit radius, shown to be approximately constant by Lecavelier des Etangs et al. (2008), and $R_{\rm P}$ is the radius of the planet.

abundance of the absorbing chemical species

Huitson et al. 2012, MNRAS, 422, 2477
Based on Lecavelier des Etangs et al. 2008, A&AL, 481, 83

Transits: Transmission Spectroscopy

HD209458b

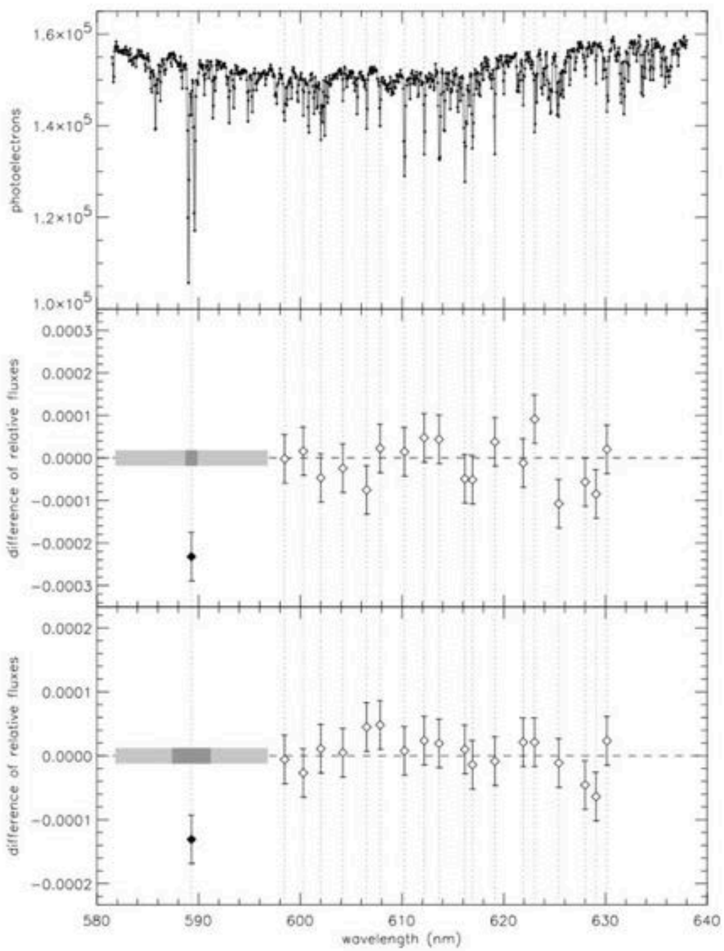

Real data

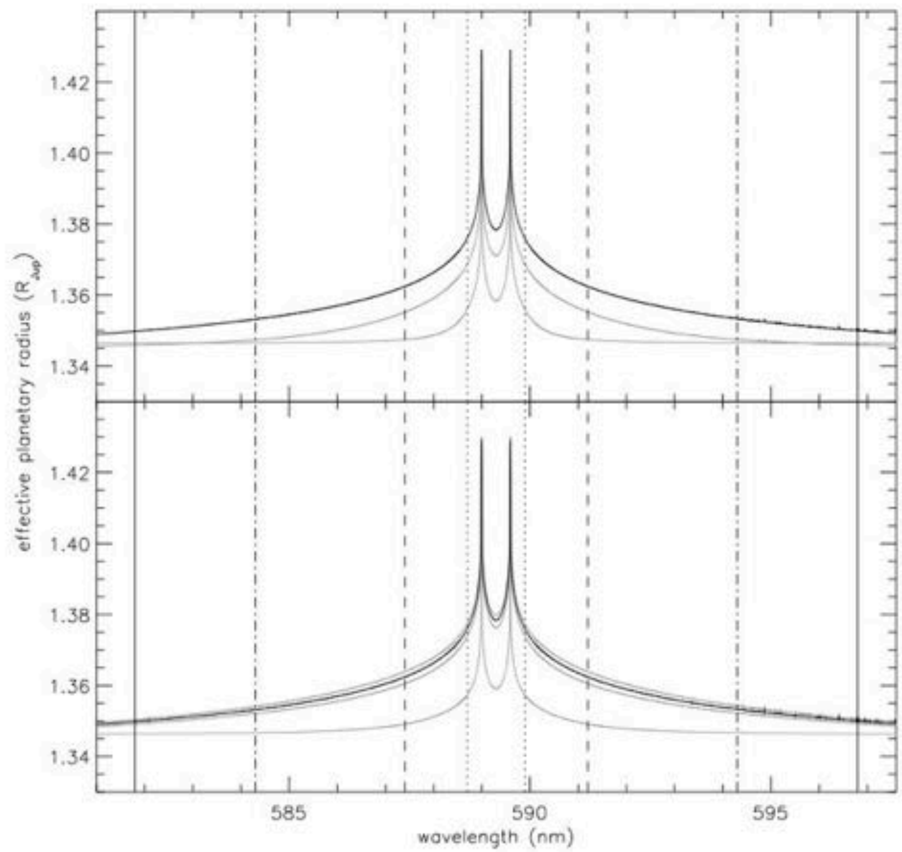

Theoretical models

Charbonneau et al. 2002, ApJ, 568, 377

Transits: Transmission Spectroscopy

Condensation

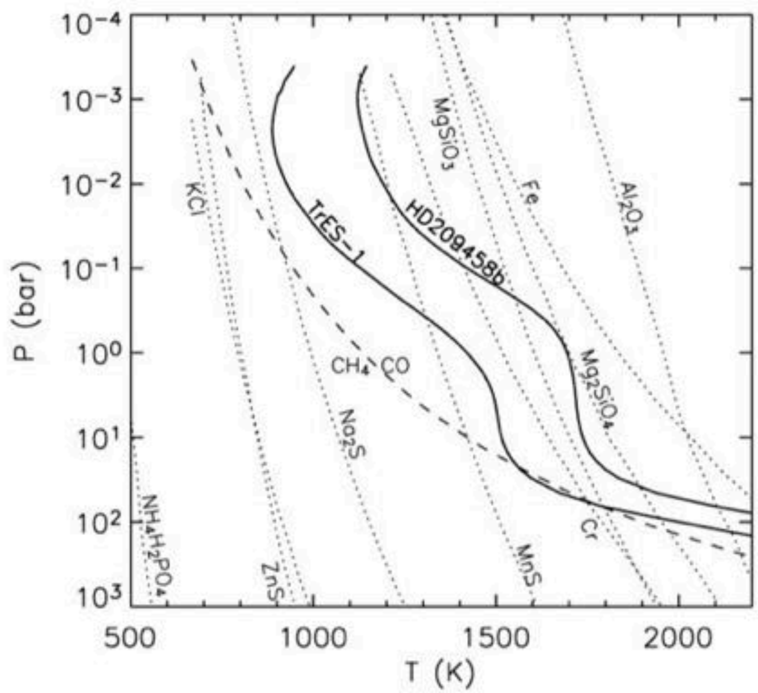

Figure 2. Pressure–temperature profiles for TrES-1 and HD 209458b. Condensation curves for various compounds, as taken from Lodders & Fegley (2005) are shown as dotted lines. The boundary where CH_4 and CO have the same abundance is shown as a dashed line.

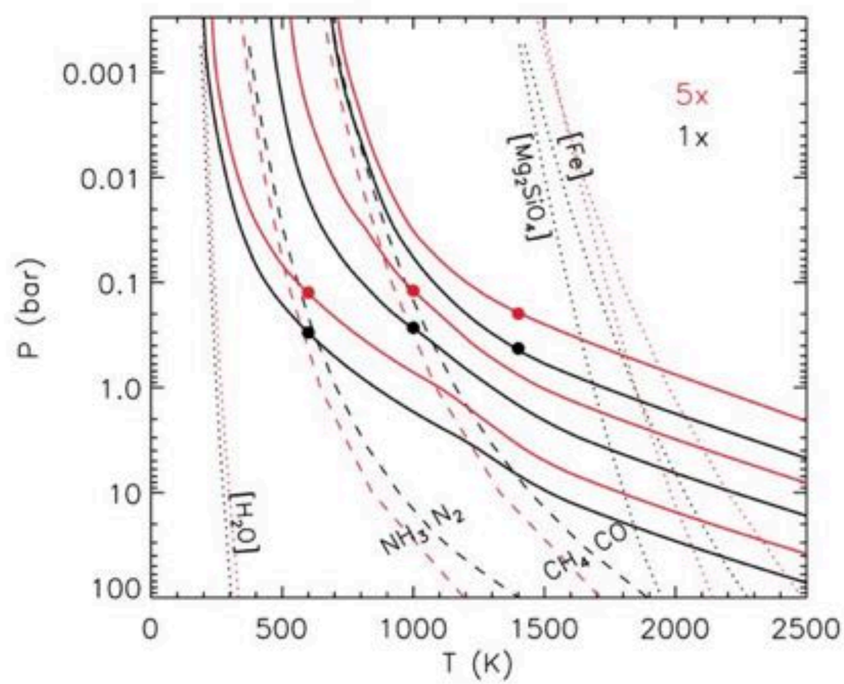

FIG. 2.—Cloud-free *P-T* profiles at 1400, 1000, and 600 K at $\log g = 3.67$. Curves in black are for 1× solar metallicity. Curves in red are for 5× solar metallicity. Circles indicate the pressure of the mean photosphere, where $T = T_{\rm eff}$. Dotted curves show locations of cloud condensation, while dashed curves are chemical equal abundance boundaries. Only the 1× boundaries (*black*) are labeled. Note that condensation curves shift to higher temperatures as metallicity increases, while equal abundance boundaries shift to lower temperatures.

Fortney 2005, MNRAS, 364, 649

Fortney et al. 2008, ApJ, 683, 1104

Transits and Occultations

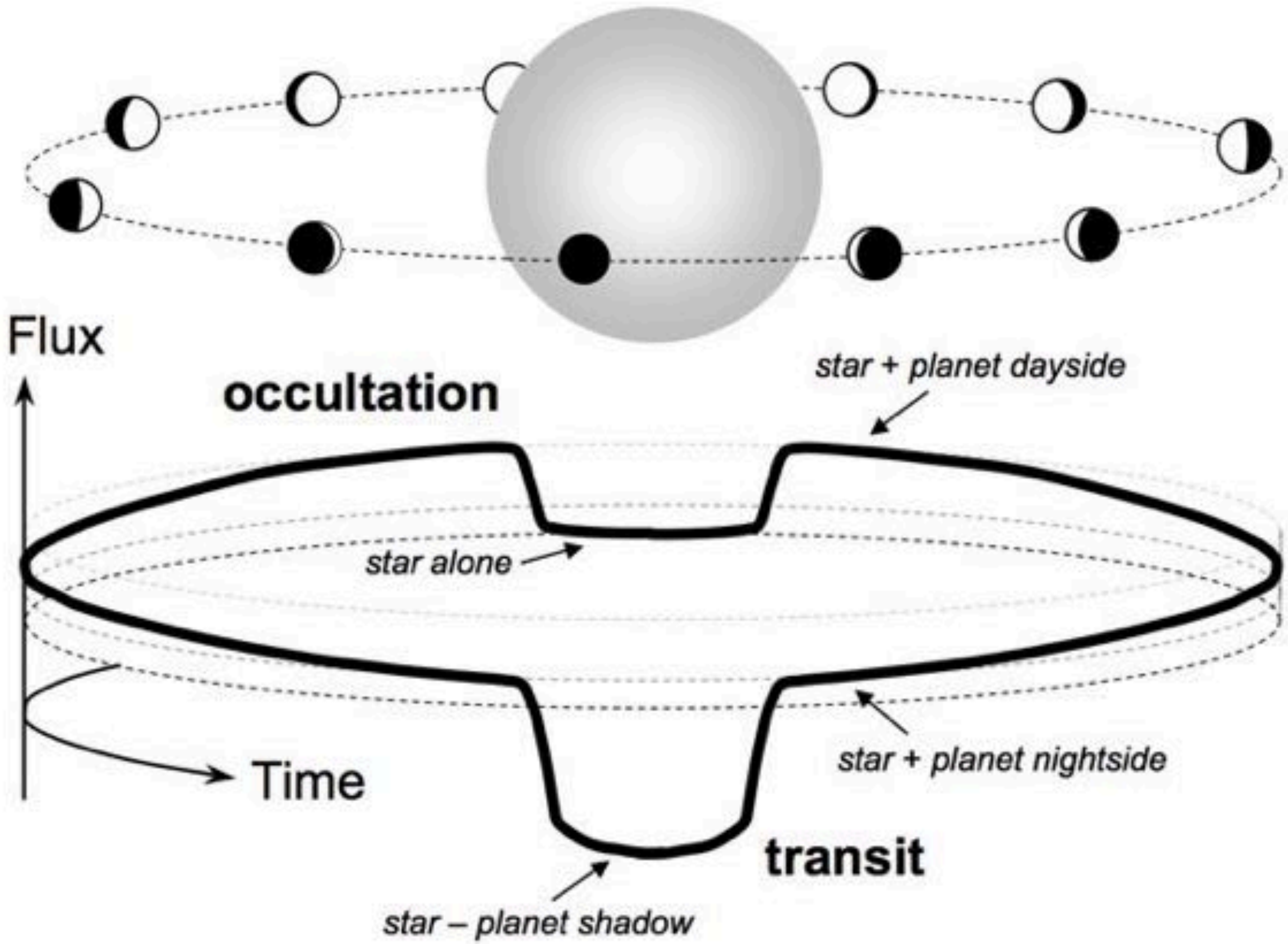

Transits: Phase-Resolved Emission Spectroscopy

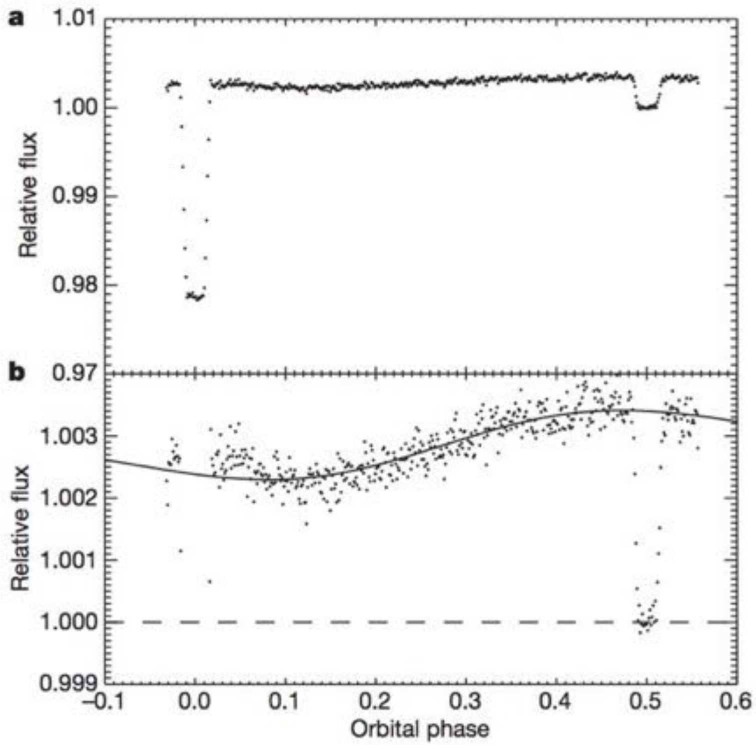

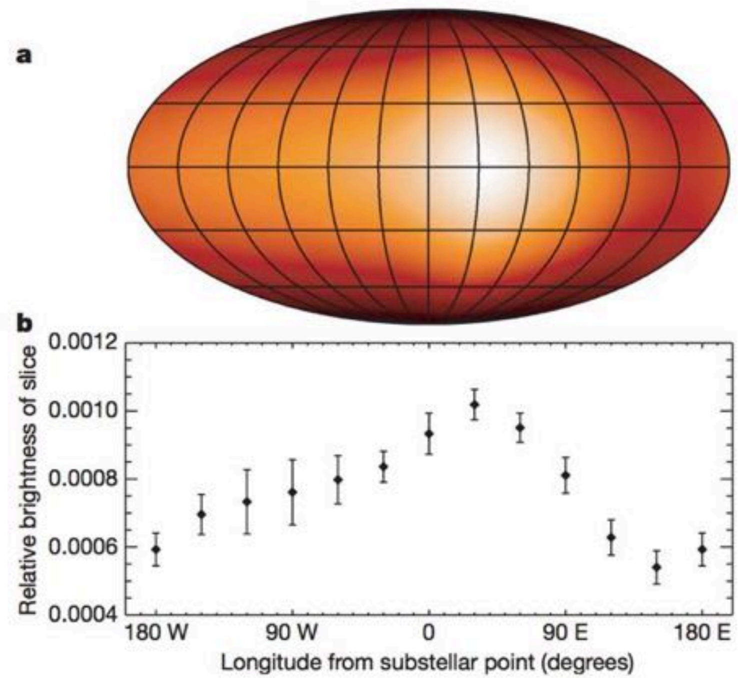

HD189733b

Real data

Knutson et al. 2007, Nature, 447, 183

Transits: Phase-Resolved Emission Spectroscopy

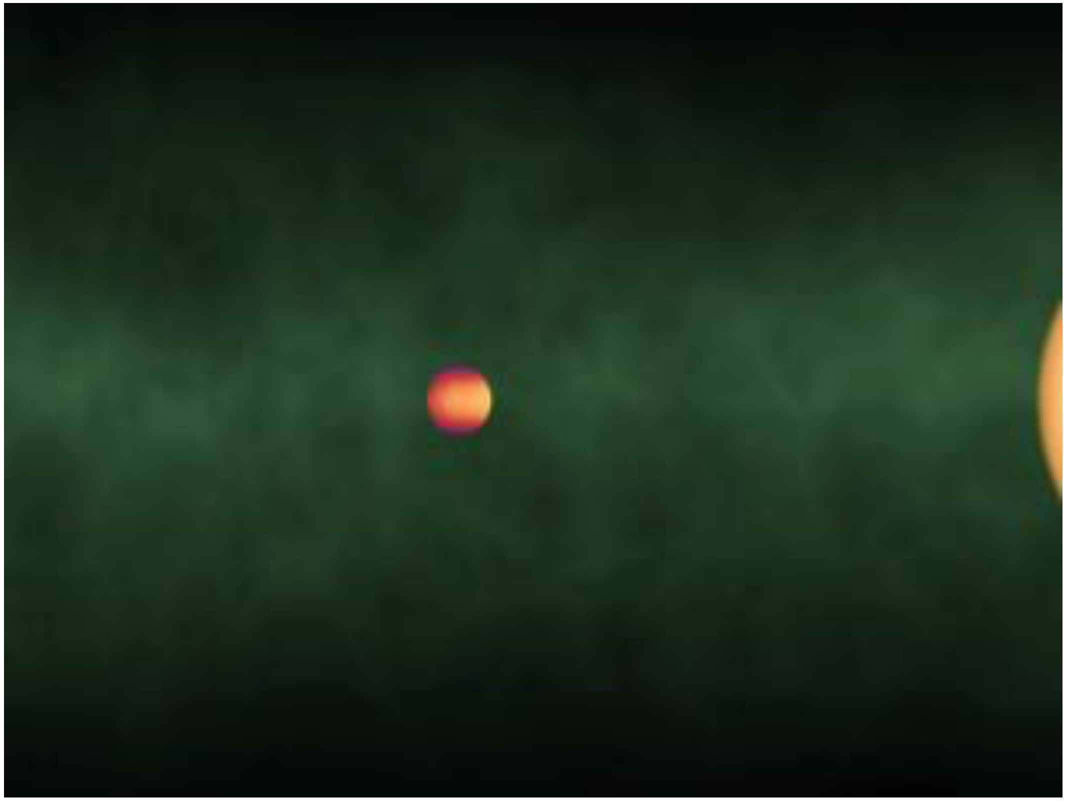

Transits: Phase-Resolved Emission Spectroscopy

Theoretical predictions using a GCM

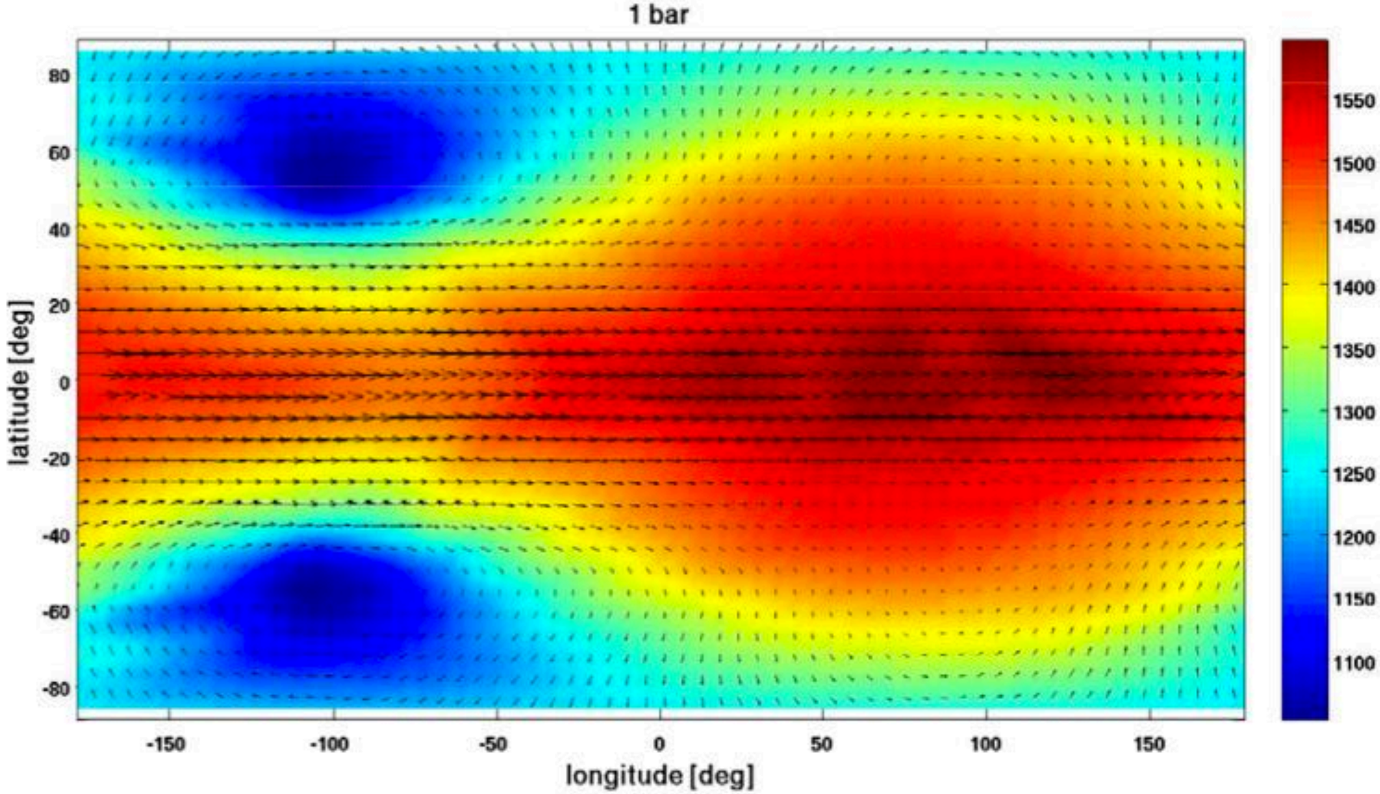

Showman et al. 2009, ApJ, 699, 564

Challenges

- Collecting enough photons
- Aperture (slit) losses
- Pointing variations + inter- and intra-pixel sensitivity variations
- Detector persistence
- Telluric transparency variations and contamination
- Limb darkening
- Stellar activity
- Mystery effects

Astronaut Andrew Feustel installs the **Wide Field Camera 3** (May 14, 2009)

Using an instrument designed for faint galaxies to look at bright, nearby stars

HST+ WFC3 spatial scan

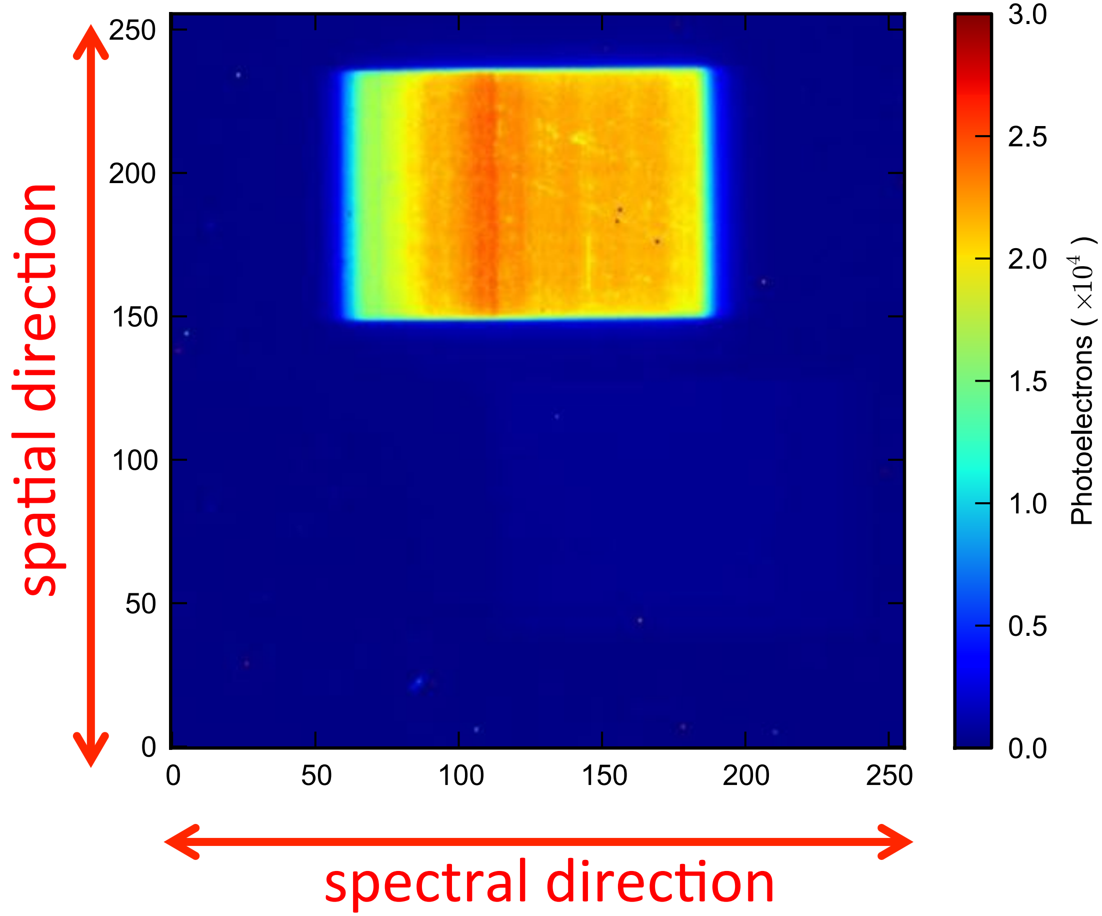

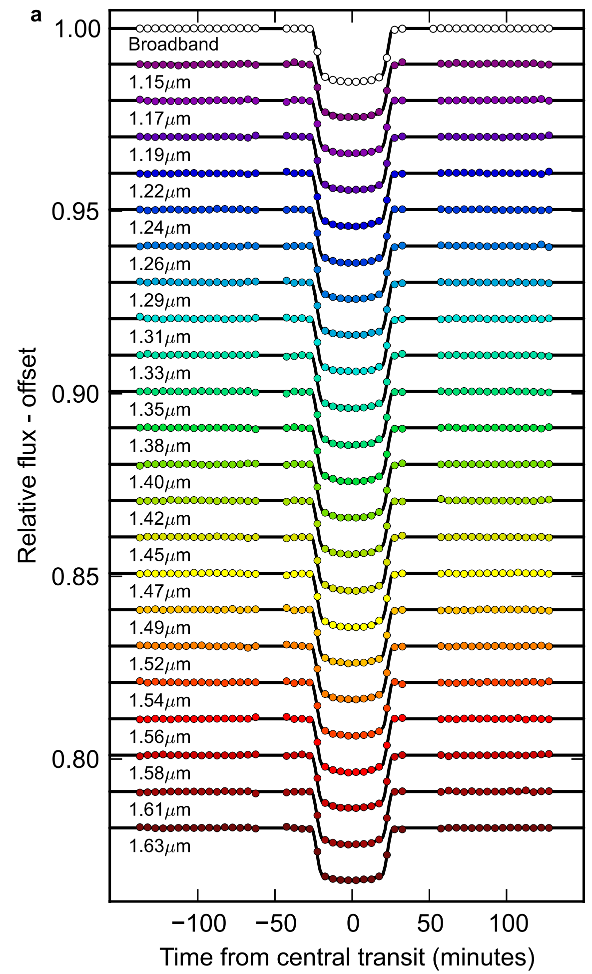

Kreidberg+ 2014a

HST+ WFC3: staring mode

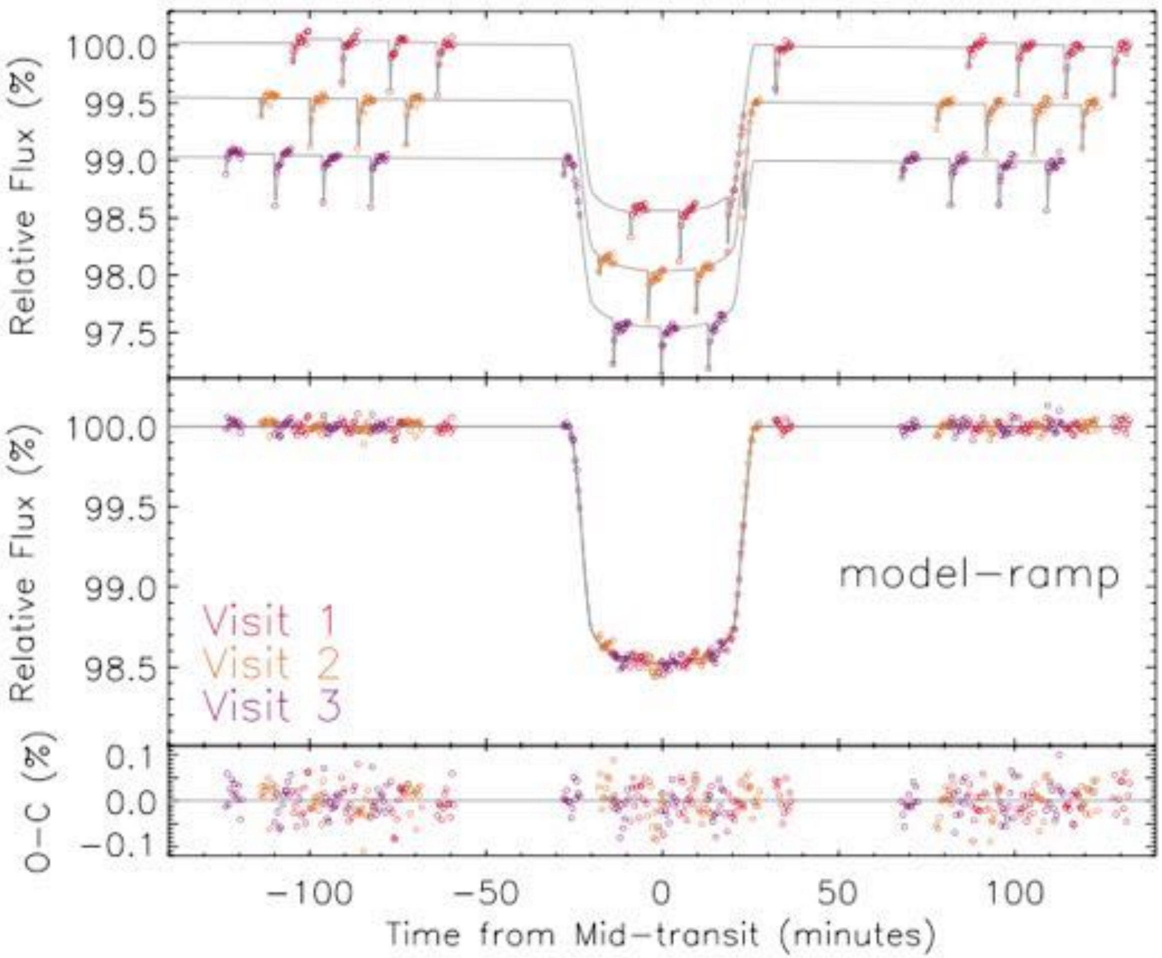

Berta+ 2012

Challenges

- Collecting enough photons
- Aperture (slit) losses
- Pointing variations + inter- and intra-pixel sensitivity variations
- Detector persistence
- Telluric transparency variations and contamination
- Limb darkening
- Stellar activity
- Mystery effects

White Light Case Study #1: HAT-P-1b

how wide do the slits have to be?

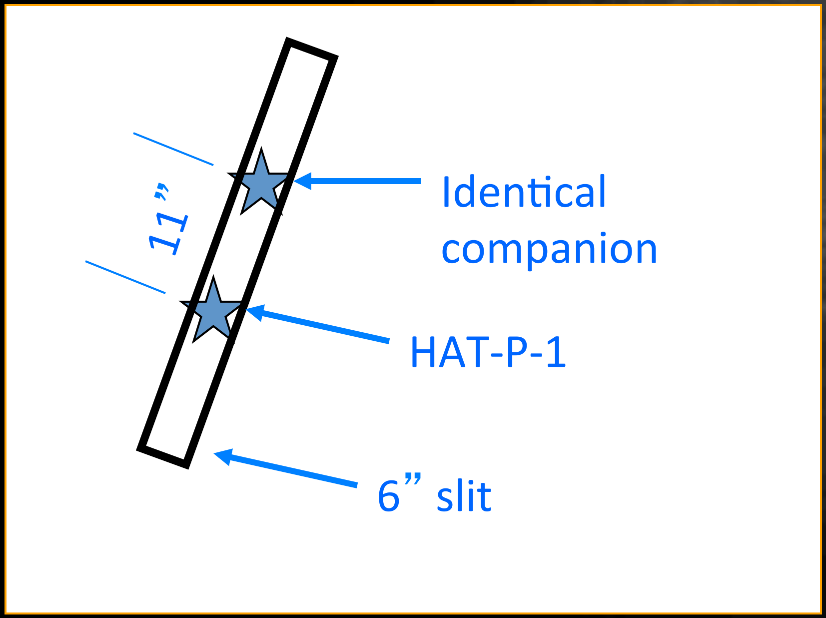

White Light Case Study #1: HAT-P-1b

how wide do the slits have to be?

Calar Alto 3.5m + TWIN

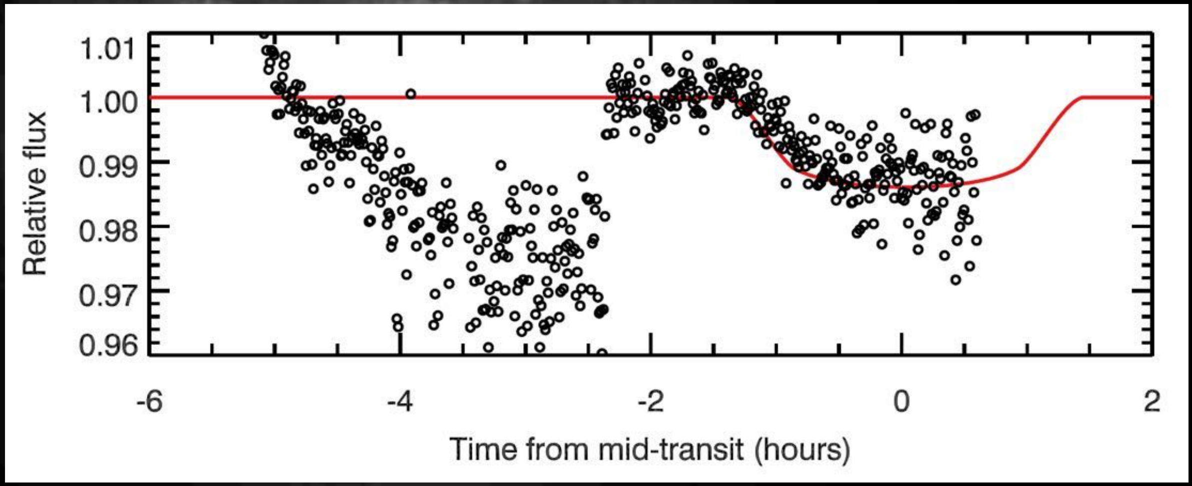

bad guiding

differential slit losses

White Light Case Study #1: HAT-P-1b

how wide do the slits have to be?

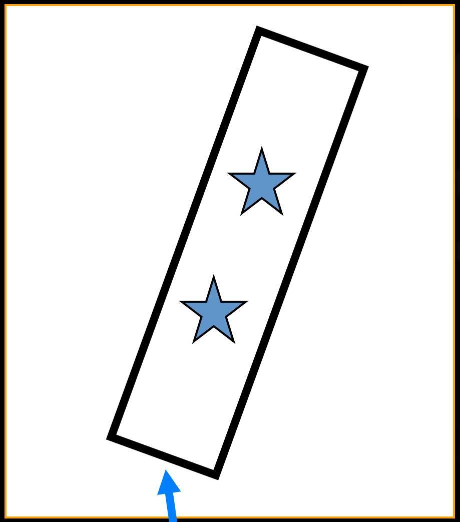

Calar Alto 3.5m + MOSCA

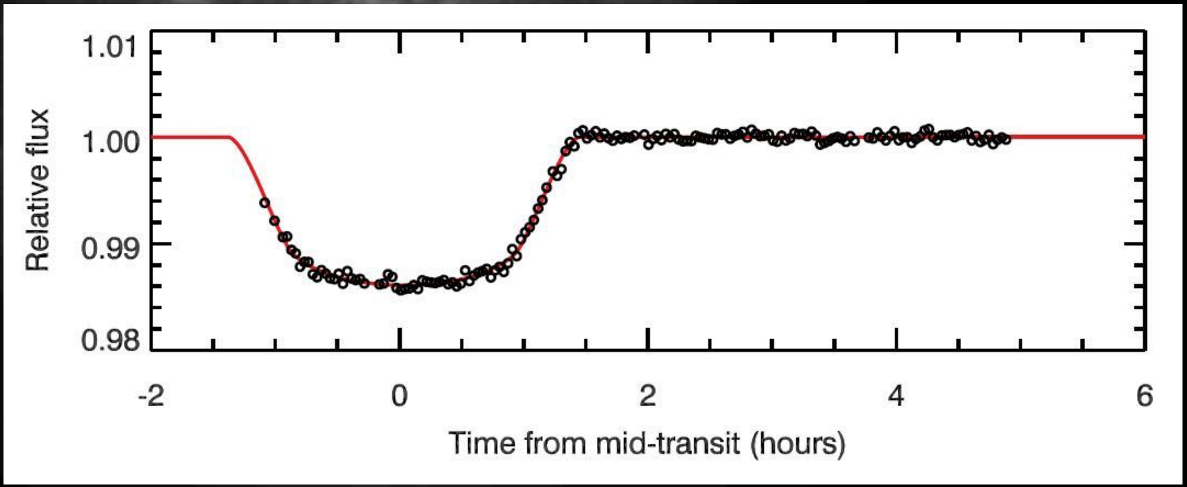

rms = 330 ppm!

(includes spatial position de-correlation)

White Light Case Study #2: GJ1214b

multi-object spectrograph – VLT + FORS

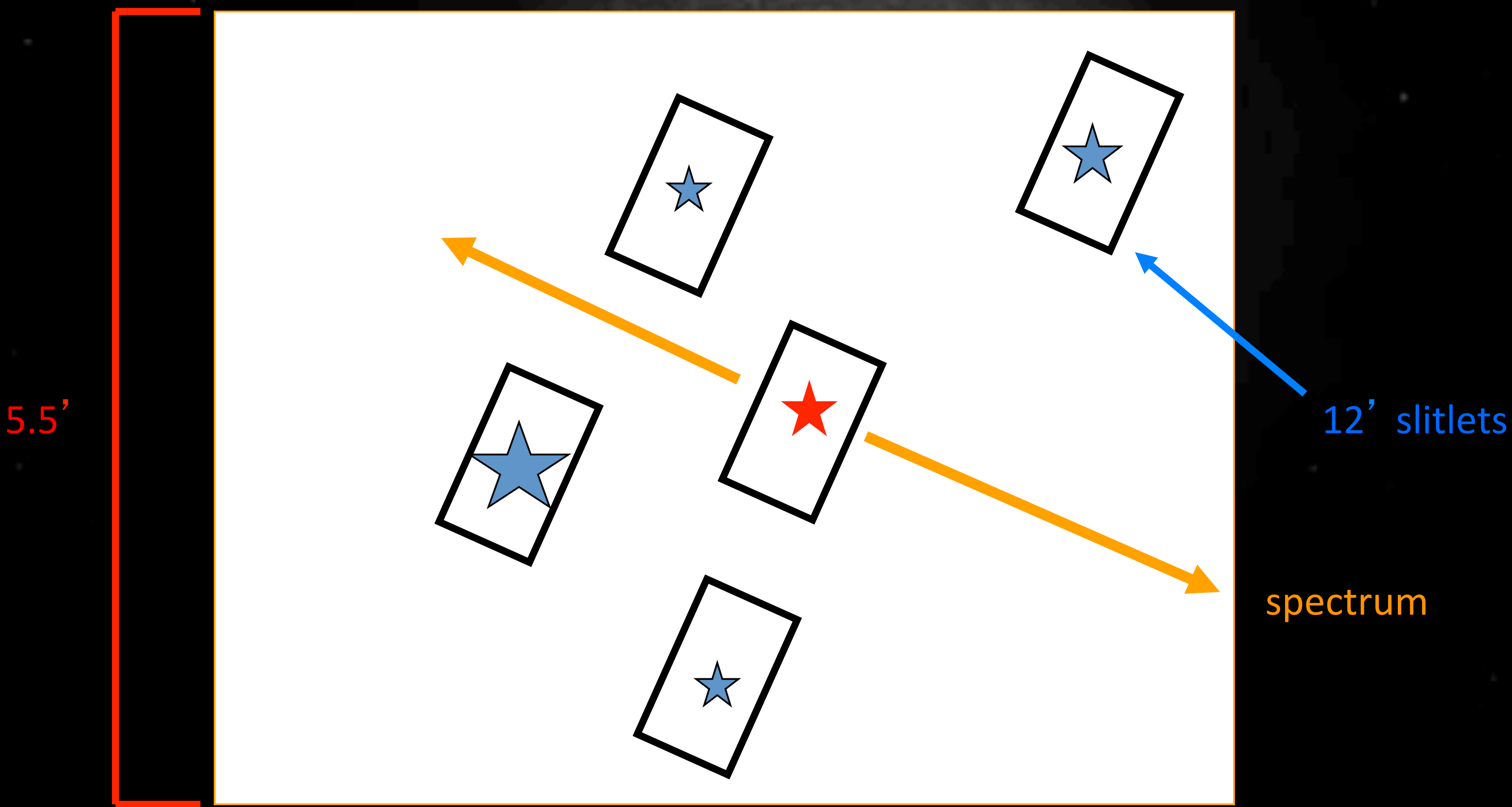

White Light Case Study #2: GJ1214b

multi-object spectrograph – VLT + FORS

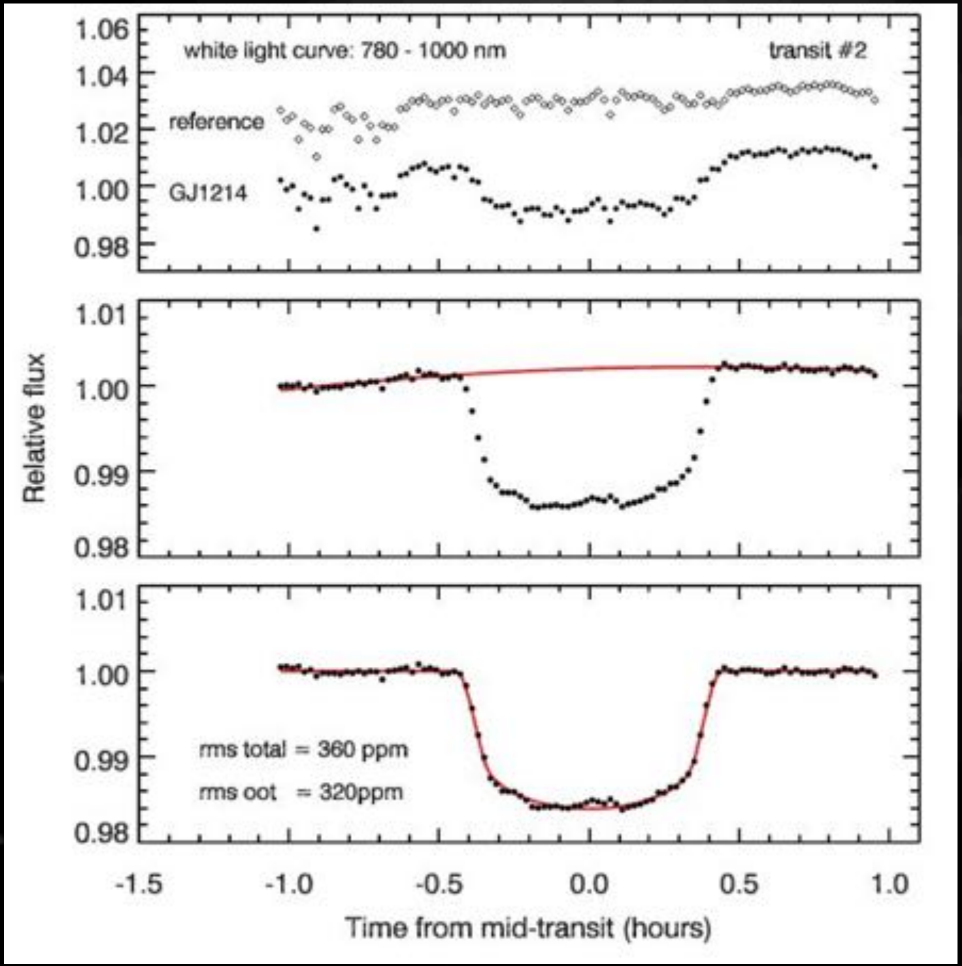

Bean+ 2010

Challenges

- Collecting enough photons
- Aperture (slit) losses
- Pointing variations + inter- and intra-pixel sensitivity variations
- Detector persistence
- Telluric transparency variations and contamination
- Limb darkening
- Stellar activity
- Mystery effects

Spitzer + IRAC

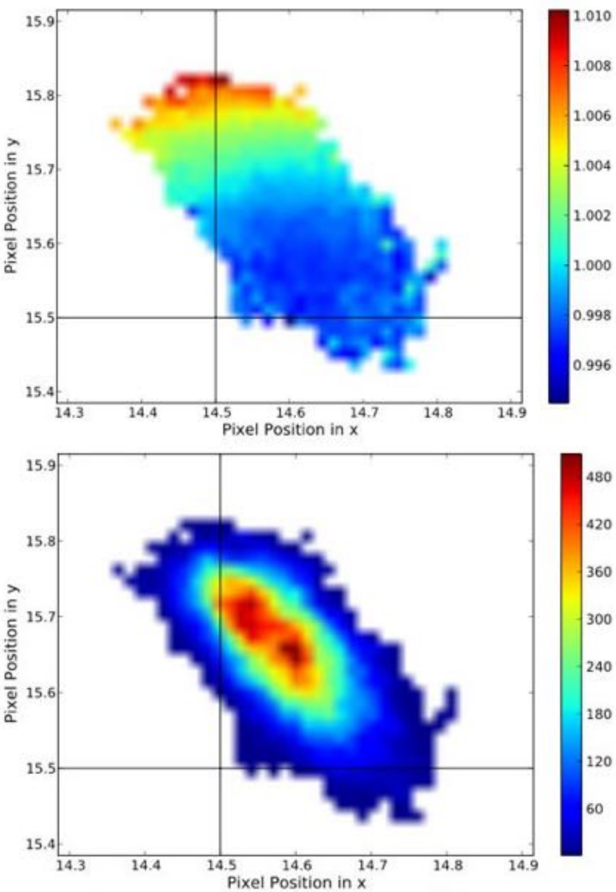

Figure 6. BLISS map and pointing histogram of HD149bs11. Top: redder (bluer) colors indicate higher (lower) subpixel sensitivity. The horizontal and vertical black lines depict pixel boundaries. Bottom: colors indicate the number of points in a given bin, which, in this case, is 0.015 pixels in length and width. By recalculating the map at each step of the MCMC or minimizer, this technique substantially improves on that of B10, and beats all tested functional fits.

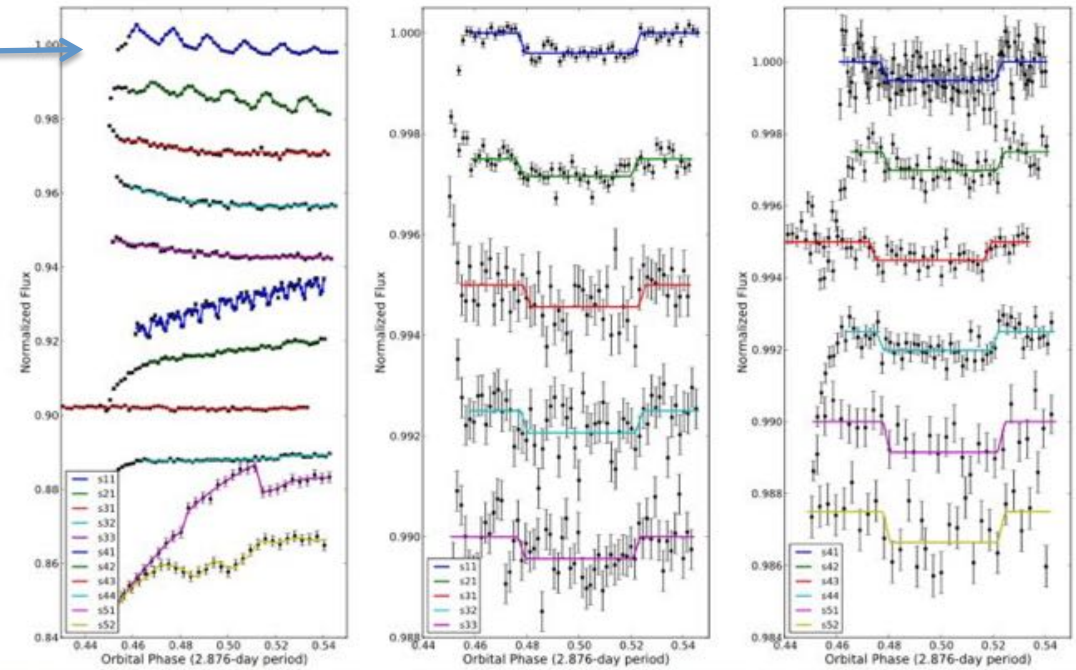

Figure 10. Binned (left) and systematics-corrected (center and right) secondary-eclipse light curves of HD 149026b in five *Spitzer* channels. The results are normalized to the system flux and shifted vertically for ease of comparison. The colored lines are best-fit models and the error bars are 1σ uncertainties. The shorthanded legend labels correspond to the last three characters in each event's label (e.g., s11 = HD149bs11).

Stevenson+ 2012

Challenges

- Collecting enough photons
- Aperture (slit) losses
- Pointing variations + inter- and intra-pixel sensitivity variations
- Detector persistence
- Telluric transparency variations and contamination
- Limb darkening
- Stellar activity
- Mystery effects

HST + WFC3

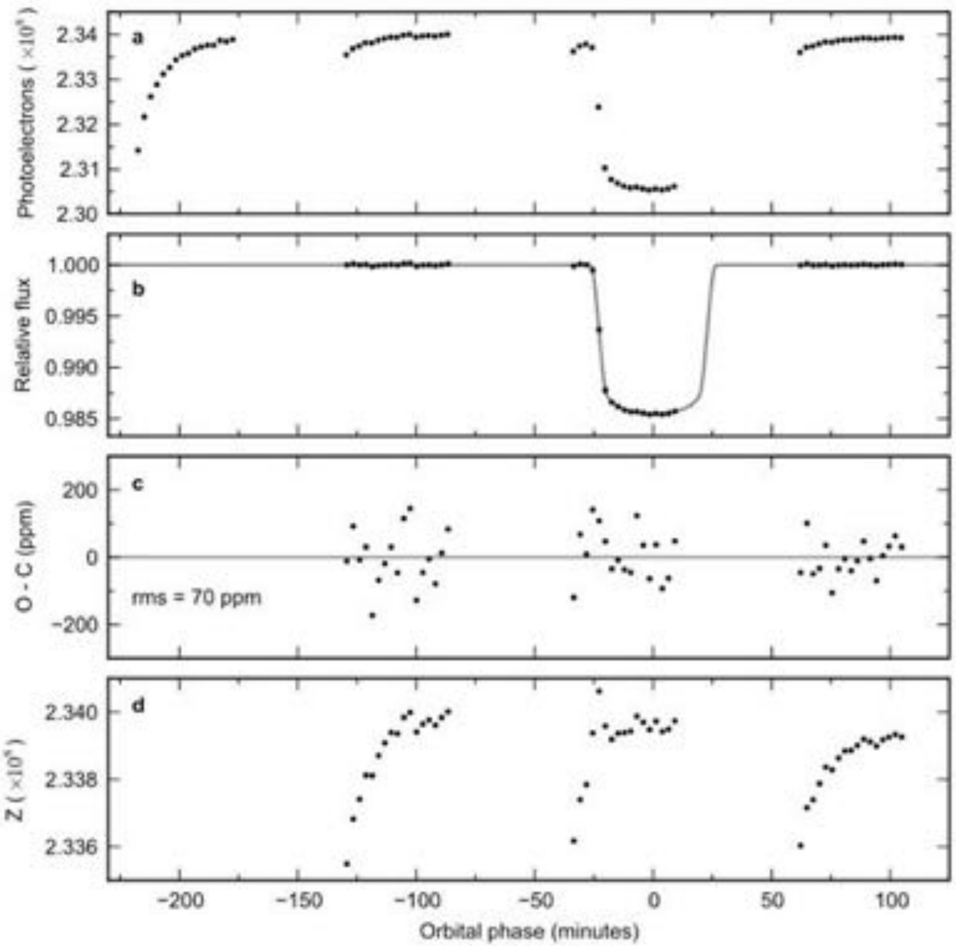

Extended Data Figure 3: **a**, The broadband light curve from the first transit observation. **b**, The broadband light curve corrected for systematics using the `model-ramp` technique (points) and the best-fit model (line). **c**, Residuals from the white light curve fit. **d**, The vector of systematics Z used in the `divide-white` technique.

Kreidberg+ 2014a

Challenges

- Collecting enough photons
- Aperture (slit) losses
- Pointing variations + inter- and intra-pixel sensitivity variations
- Detector persistence
- Telluric transparency variations and contamination
- Limb darkening
- Stellar activity
- Mystery effects

VLT + CRIRES

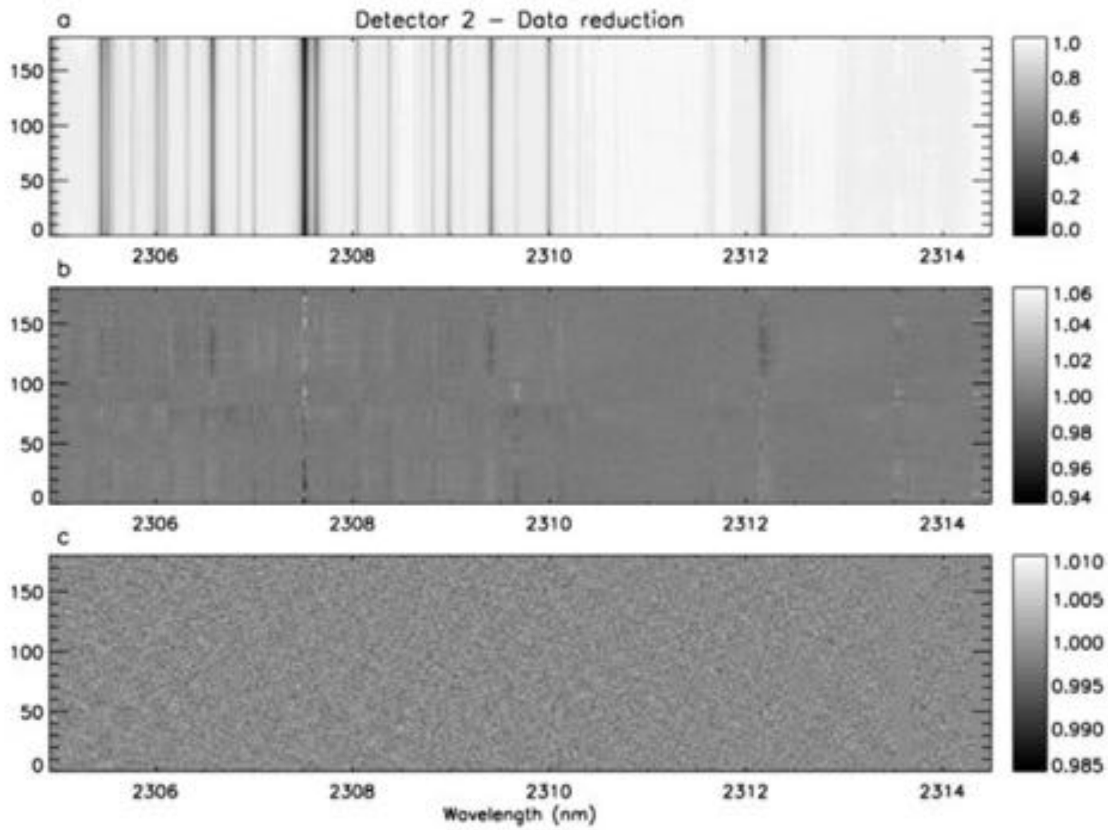

Fig. S2: An example of our data reduction chain, showing the spectral series from CRIRES detector #2, taken on April 1, 2011. The y-axis corresponds to time. Data are first aligned and normalized to the same continuum level (a), and subsequently de-trended from the effects of the geometric airmass (b). Finally, correlated and low-order residuals are removed and bad regions in the array are masked (c). See section SI-2.2 for further details.

Brogi+ 2012

Challenges

- Collecting enough photons
- Aperture (slit) losses
- Pointing variations + inter- and intra-pixel sensitivity variations
- Detector persistence
- Telluric transparency variations and contamination
- Limb darkening
- Stellar activity
- Mystery effects

GJ 1214b with *HST* + WFC3

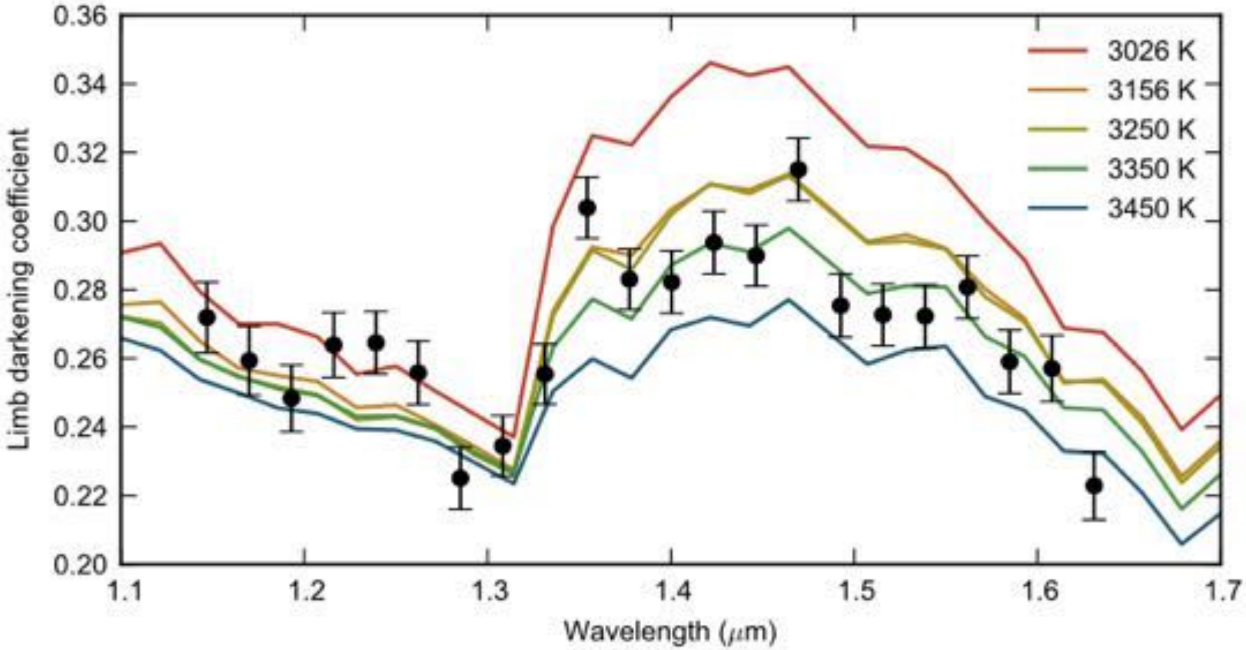

Extended Data Figure 6: Fitted limb darkening coefficients as a function of wavelength (black points) and theoretical predictions for stellar atmospheres with a range of temperatures (lines). The uncertainties are 1 σ confidence intervals from an MCMC. The temperature of GJ 1214 is estimated to be 3250 K[22].

Kreidberg+ 2014a

Challenges

- Collecting enough photons
- Aperture (slit) losses
- Pointing variations + inter- and intra-pixel sensitivity variations
- Detector persistence
- Telluric transparency variations and contamination
- Limb darkening
- Stellar activity
- Mystery effects

Stellar activity for HD 189733b?

Figure 4. Transmission spectrum of the exoplanet HD 189733b. Observations: data from Table 3 of this work, binned to seven points, are indicated by the filled black circles connected by a line. The WFC3 spectrum's S-shaped undulation is attributed to water vapor (see Figure 5). Except for the WFC3 spectrum, all of the data and associated uncertainties are from Table 5 of Pont et al. (2013), including spectroscopy (filled colored circles) and photometry (open colored squares). As such, the illustrated NICMOS spectrum was reported originally by Gibson et al. (2011) and has a median uncertainty per point of 234 ppm. The median uncertainty per point estimated by three different analyses of those same NICMOS data ranges from 80 ppm to 234 ppm, although the shapes of the independently derived spectra are similar (Swain et al. 2014). Data from Table 3 of Sing et al. (2011) include five pairs of points from the G430L grating of STIS (open violet circles), except their wavelengths have been reduced 2% for clarity. Data from Table 2 of Pont et al. (2008) include 10 points from the G800L grating of ACS (open blue circles). Different corrections to the same data account for the different transit depths (open vs. filled circles; $\lambda < 1.7\,\mu$m). Uncertainties are represented by 1σ error bars. Transitions of atomic sodium and potassium are indicated. Models: the blue dashed line is a fit to the Pont et al. (2008) data (open blue circles) by Lecavelier Des Etangs et al. (2008a) with a model of a clear, Rayleigh-scattering planetary atmosphere of the form of Equation (1) of Lecavelier Des Etangs et al. (2008b). The blue solid line is the same fit, shifted down to match the data of Pont et al. (2013) (filled blue circles). The orange lines have a fixed planetary radius R_p and blackbody stellar models with unocculted star spots. The temperature of the stellar photosphere is 5000 K. The modeled spot temperatures and covering fractions are 4600 K and 0.08 (solid), and 3700 K and 0.056 (dashed). Both spot models have been normalized at $\lambda = 24\,\mu$m to match the MIPS data point. An annulus of radius equal to R_p and width equal to a single $T = 1200$ K pressure scale height ($H = 193$ km) corresponds to 112 ppm of transit depth, as indicated by the right scale.

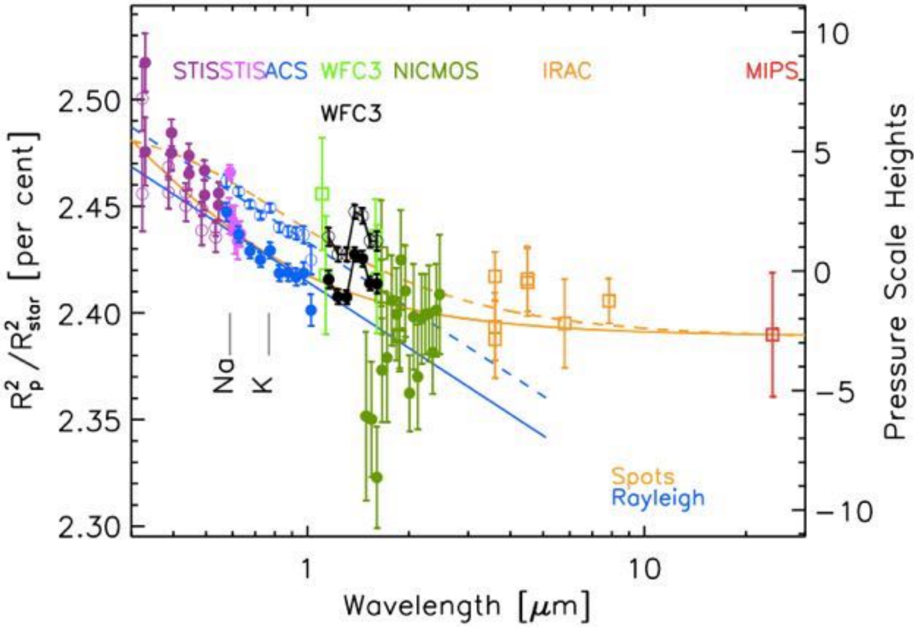

McCullough+ 2014

Challenges

- Collecting enough photons
- Aperture (slit) losses
- Pointing variations + inter- and intra-pixel sensitivity variations
- Detector persistence
- Telluric transparency variations and contamination
- Limb darkening
- Stellar activity
- Mystery effects

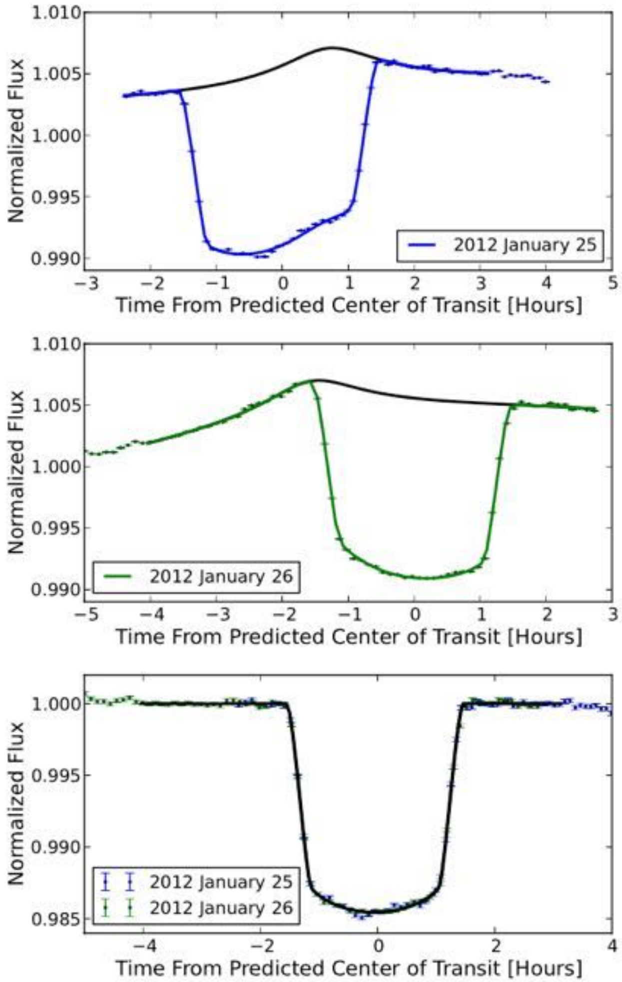

Figure 3. White light curves and best-fit transit models of WASP-12b. The upper and middle panels depict light curves of WASP-12 from 2012 January 25 and 26, respectively, that are binned in pairs and corrected for atmospheric variations using a comparison star. We model the instrument-related systematic using Equation (1) and apply the full model given by Equation (2). We do not use flux from 720 to 765 nm to construct the white light curves because of an anomalous increase in flux toward the end of each observation, as discussed in Section 2.4. We exclude points that are far from each transit because the systematic models provide a less-than-ideal fit to these data, which can skew the best-fit transit parameters. The lower panel presents the normalized, systematics-removed light curves with 1σ uncertainties and a best-fit transit model in black. The residual rms value for each white light curve is 180 ppm and uncertainties are $3.1\times$ the photon limit.

Gemini + GMOS

Stevenson+ 2014a

HST + WFC3

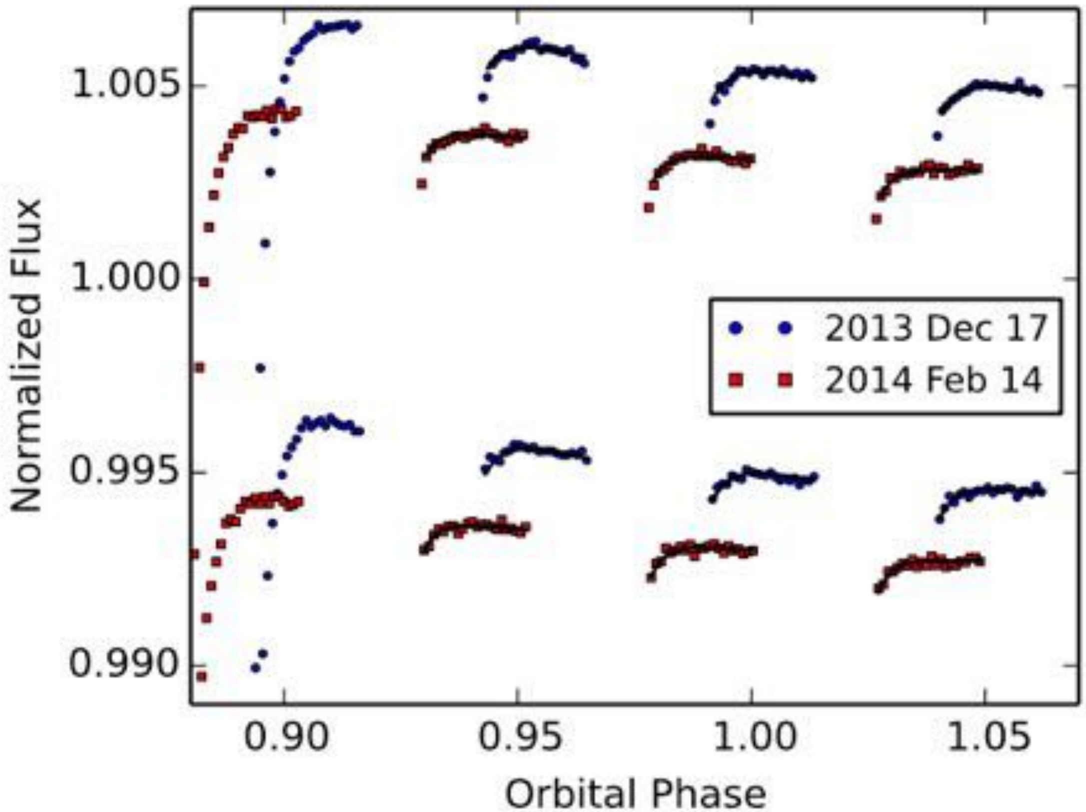

Figure 1. *HST*/WFC3 white light curves of GJ 436. Blue circles depict the 2013 December 17 data set and red squares depict the 2014 February 14 data set. Typical per point uncertainties are the size of the symbols (67 ppm). For comparison, we include sample models (black curves) that fit orbits 2–4 and exclude the first point from each orbit. The forward and reverse scan directions produce the observed 1% flux offset within each data set.

Stevenson+ 2014b

The potential of *JWST* for transit spectroscopy

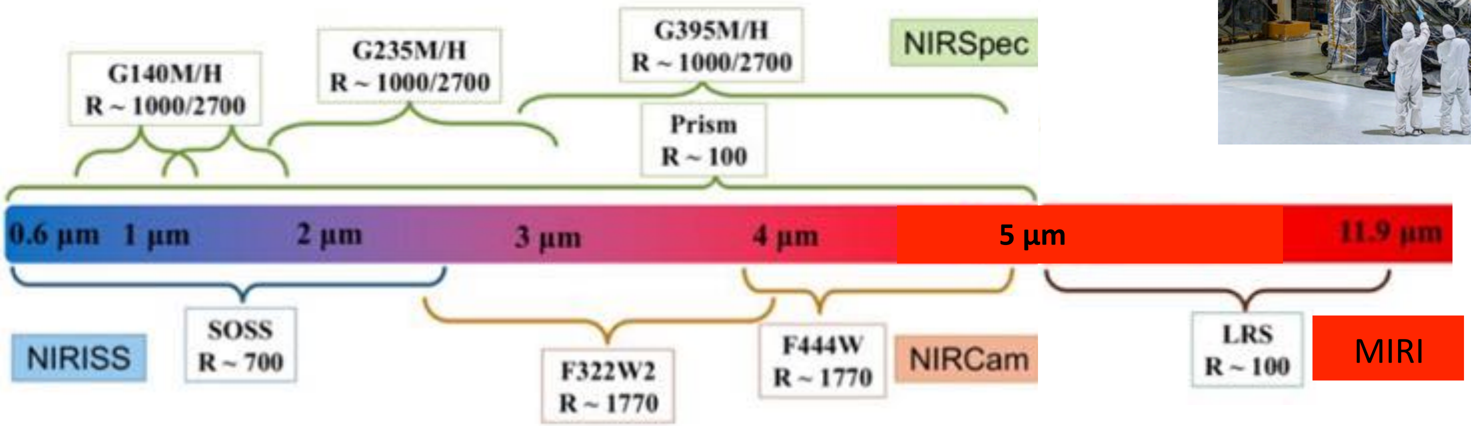

JWST Director's Discretionary Early Release Science Call for Proposals

Last Updated Jul 25, 2017

James Webb Space Telescope User Documentation

HOME | INSTRUMENTS | PLANNING | CALL FOR PROPOSALS | POLICIES | DATA | Search

JWST Opportunities and Policies / JWST Cycle 1 Proposal Opportunities

JWST Director's Discretionary Early Release Science Call for Proposals

Last Updated Jul 25, 2017

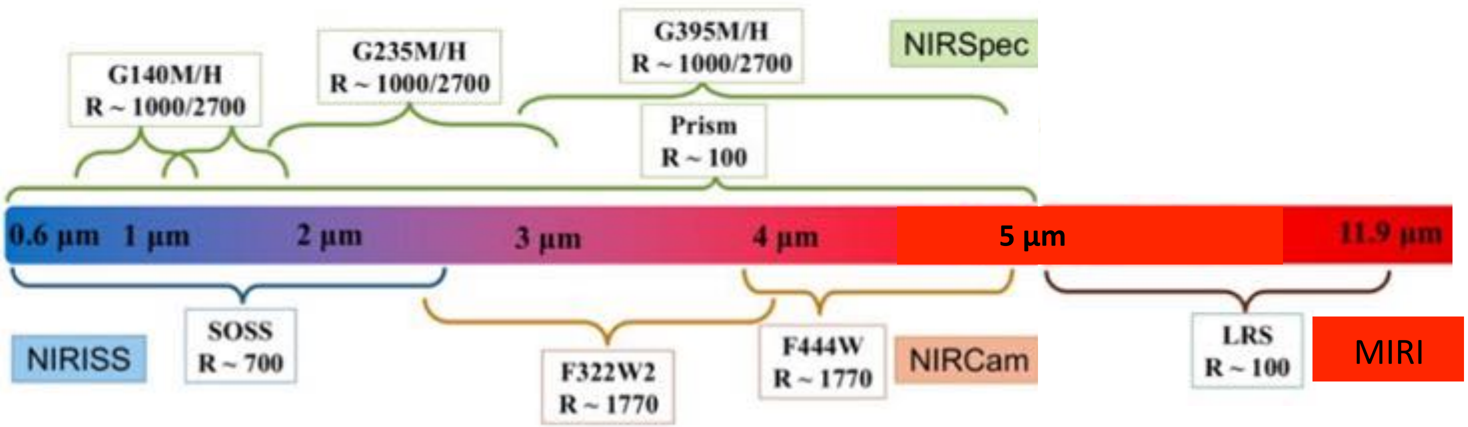

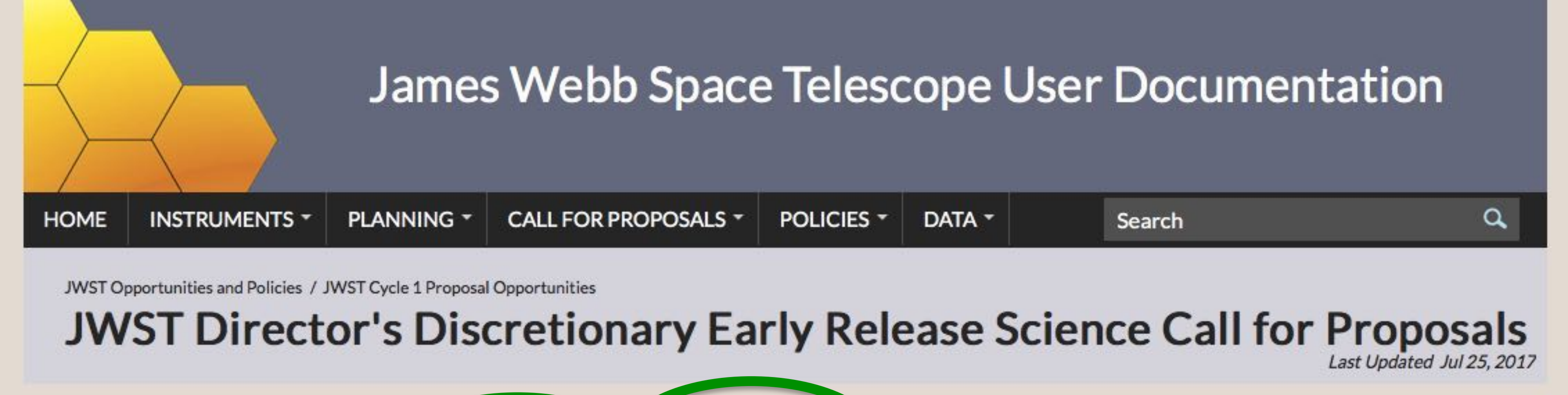

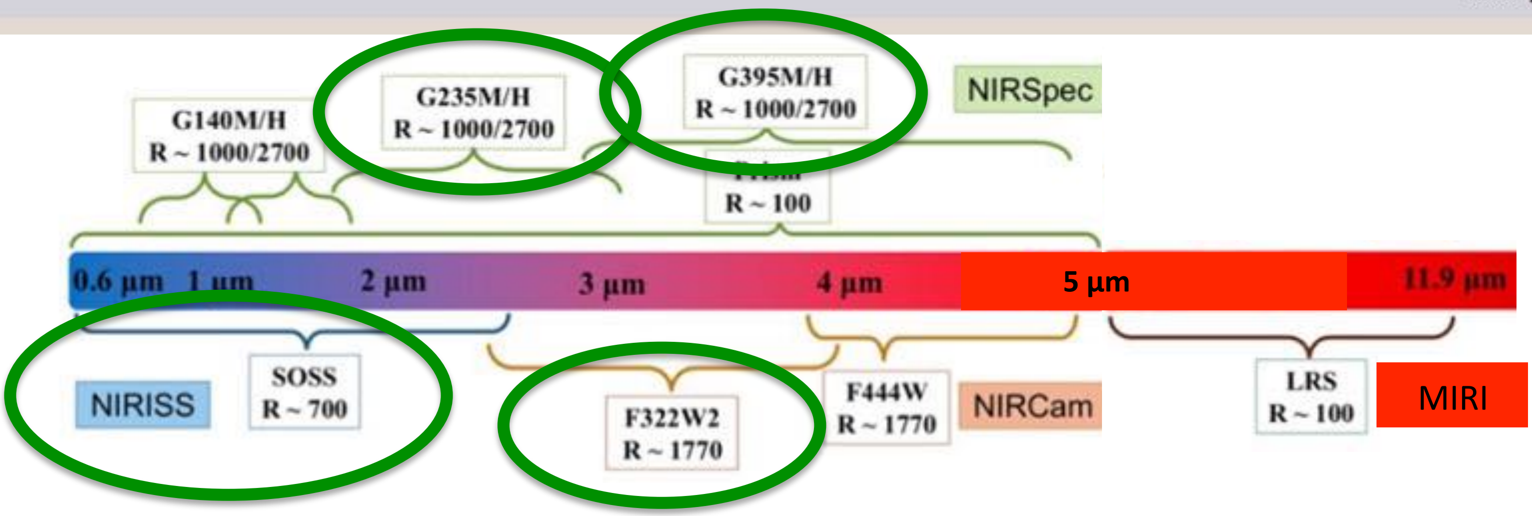

Transmission spectroscopy

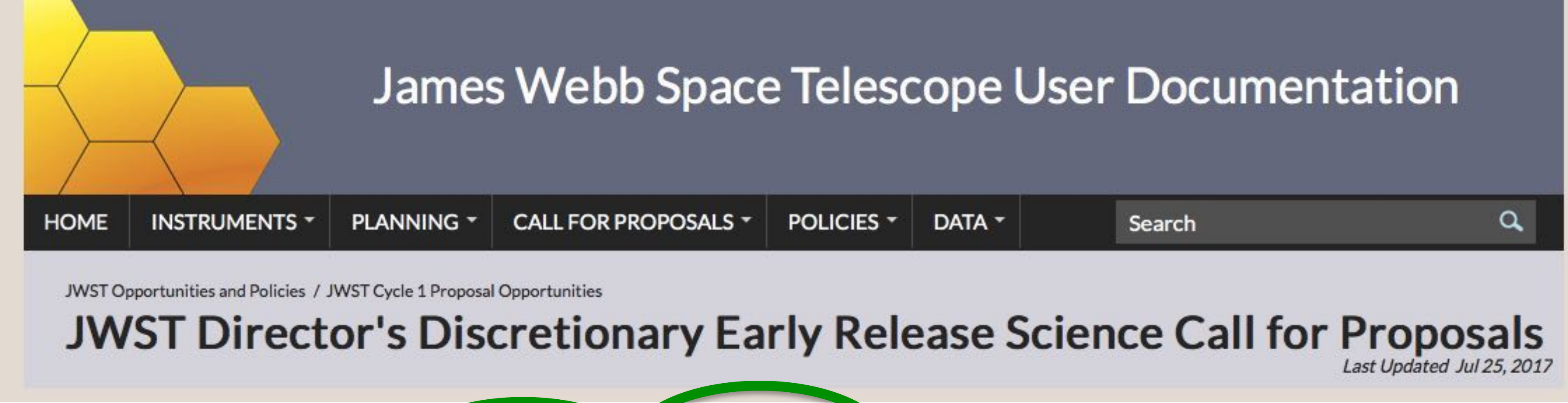

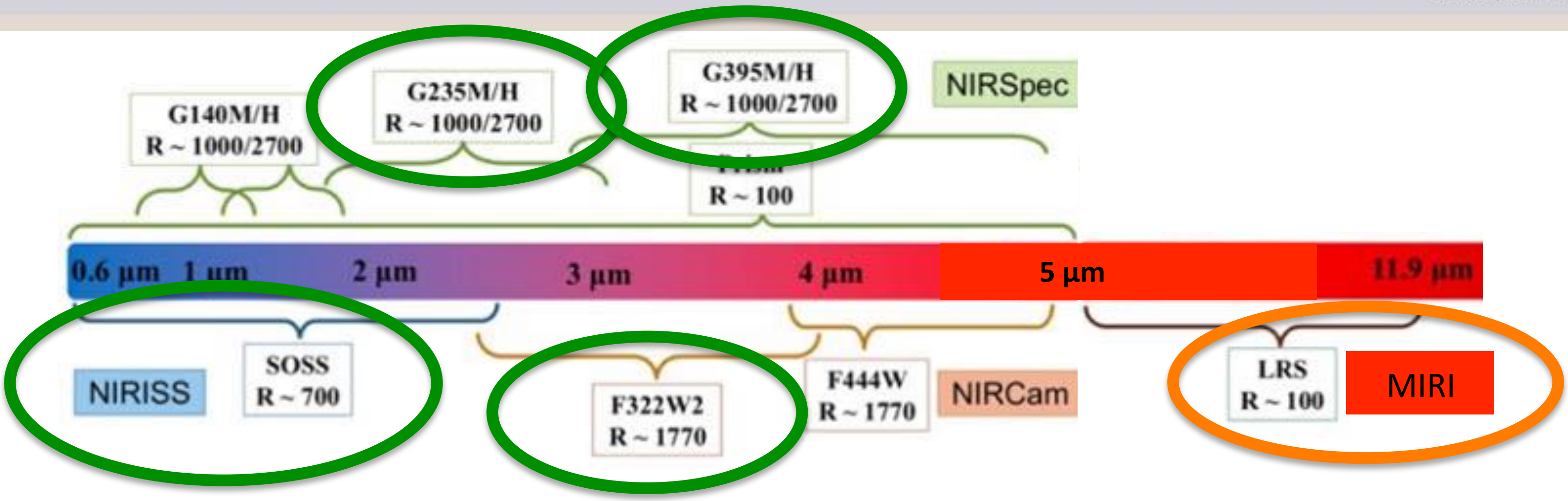

Transmission spectroscopy

Full orbit phase curve (with two secondary eclipses)

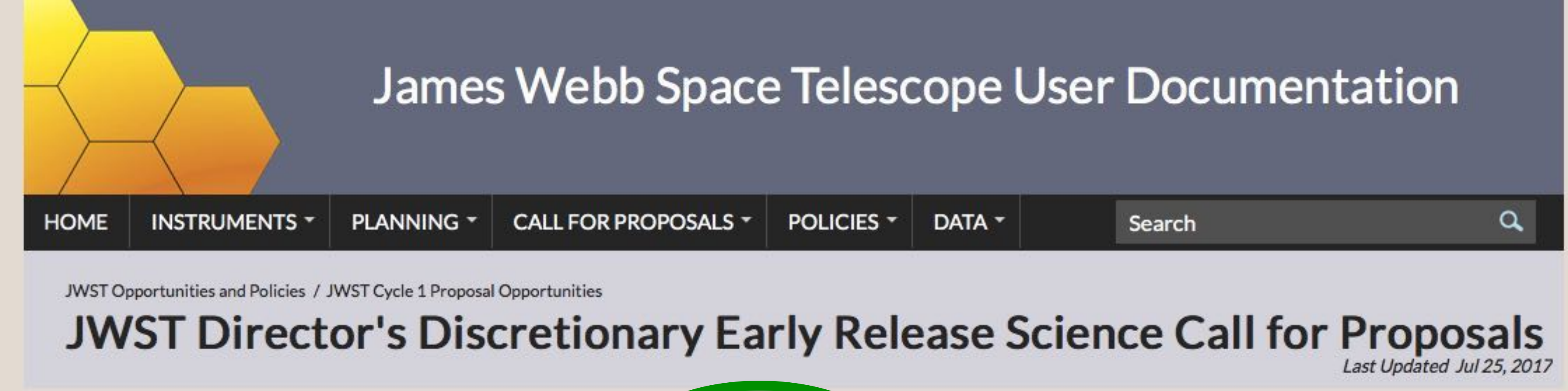

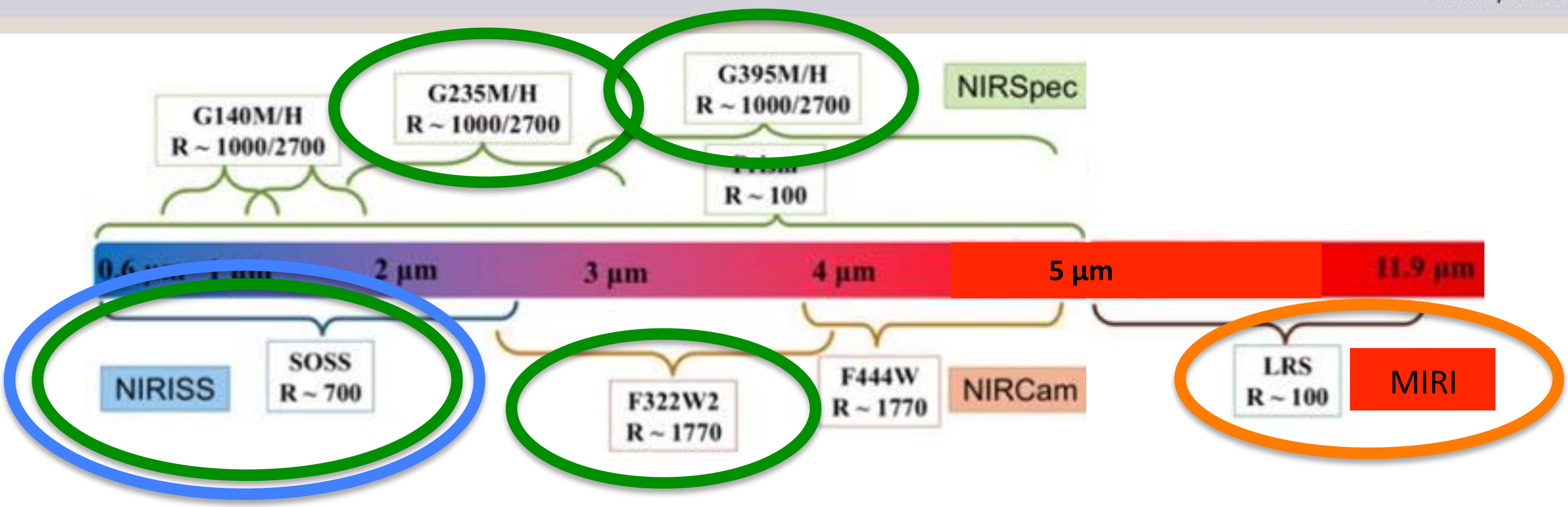

Transmission spectroscopy

Full orbit phase curve (with two secondary eclipses)

Secondary eclipse of a bright star

http://exoctk.readthedocs.io/en/latest/